

1 **Seasonal and diurnal variations of methane and carbon dioxide in the Kathmandu Valley**
2 **in the foothills of the central Himalaya**

3 Khadak Singh Mahata^{1,2}, Arnico Kumar Panday^{3,4}, Maheswar Rupakheti^{1,5*}, Ashish Singh¹,
4 Manish Naja⁶, Mark G. Lawrence^{1,2}

5 [1] Institute for Advanced Sustainability Studies (IASS), Potsdam, Germany

6 [2] University of Potsdam, Potsdam, Germany

7 [3] International Centre for Integrated Mountain Development (ICIMOD), Lalitpur, Nepal

8 [4] University of Virginia, Virginia, USA

9 [5] Himalayan Sustainability Institute (HIMSI), Kathmandu, Nepal

10 [6] Aryabhata Research Institute of Observational Sciences (ARIES), Nainital, India

11

12 *Correspondence to: M. Rupakheti (maheswar.rupakheti@iass-potsdam.de)

13

14 **Abstract**

15 The SusKat-ABC (Sustainable Atmosphere for the Kathmandu Valley- Atmospheric Brown
16 Clouds) international air pollution measurement campaign was carried out during December
17 2012-June 2013 in the Kathmandu Valley and surrounding regions in Nepal. The Kathmandu
18 Valley is a bowl-shaped basin with a severe air pollution problem. This paper reports
19 measurements of two major greenhouse gases (GHGs), methane (CH₄) and carbon dioxide
20 (CO₂), along with the pollutant CO, that began during the campaign and were extended for a year
21 at the SusKat-ABC supersite in Bode, a semi-urban location in the Kathmandu Valley.
22 Simultaneous measurements were also made during 2015 in Bode and a nearby rural site
23 (Chanban), ~25 km (aerial distance) to the southwest of Bode, on the other side of a tall ridge.
24 The ambient mixing ratios of methane (CH₄), carbon dioxide (CO₂), water vapor, and carbon
25 monoxide (CO) were measured with a cavity ring down spectrometer (Picarro G2401, USA),

26 along with meteorological parameters for a year (March 2013 - March 2014). These
27 measurements are the first of their kind in the central Himalayan foothills. At Bode, the annual
28 average mixing ratios of CO₂ and CH₄ were 419.34(±6.0) ppm and 2.192(±0.066) ppm,
29 respectively. These values are higher than the levels observed at background sites such as Mauna
30 Loa, USA (CO₂: 396.8 ± 2.0 ppm, CH₄: 1.831 ± 0.110 ppm) and Waliguan, China (CO₂: 397.7 ±
31 3.6 ppm, CH₄: 1.879 ± 0.009 ppm) during the same period, and at other urban/semi-urban sites in
32 the region such as Ahmedabad and Shadnagar (India). They varied slightly across the seasons at
33 Bode, with seasonal average CH₄ mixing ratios being 2.157(±0.230) ppm in the pre-monsoon
34 season, 2.199(±0.241) ppm in the monsoon, 2.210(±0.200) ppm in the post-monsoon, and
35 2.214(± 0.209) ppm in the winter season. The average CO₂ mixing ratios were 426.2(±25.5) ppm
36 in pre-monsoon, 413.5(±24.2) ppm in monsoon, 417.3(±23.1) ppm in post-monsoon, and
37 421.9(±20.3) ppm in winter season. The maximum seasonal mean mixing ratio of CH₄ in winter
38 was only 0.057 ppm or 2.6% higher than the seasonal minimum during the pre-monsoon period,
39 while CO₂ was 12.8 ppm or 3.1% higher during the pre-monsoon period (seasonal maximum)
40 than during the monsoon (seasonal minimum). On the other hand, the CO mixing ratio at Bode
41 was 191% higher during the winter than during the monsoon season. The enhancement in CO₂
42 mixing ratios during the pre-monsoon season is associated with additional CO₂ emissions from
43 forest fire and agro-residue burning in northern South Asia in addition to local emissions in the
44 Kathmandu Valley. Published CO/CO₂ ratios of different emission sources in Nepal and India
45 were compared with the observed CO/CO₂ ratios in this study. This comparison indicated that
46 the major sources in the Kathmandu Valley were residential cooking and vehicle exhaust in all
47 seasons except winter. In winter, the brick kiln emissions were a major source. Simultaneous
48 measurement in Bode and Chanban (15 July-3 Oct 2015) revealed that the mixing ratio of CO₂,
49 CH₄ and CO mixing ratios were 3.8%, 12%, and 64% higher in Bode than Chanban. Kathmandu
50 Valley, thus, has significant emissions from local sources, which can also be attributed to its
51 bowl shaped geography that is conducive to pollution build-up. At Bode, all three gas species
52 (CO₂, CH₄ and CO) showed strong diurnal patterns in their mixing ratios with a pronounced
53 morning peak (ca. 08:00), a dip in the afternoon, and again gradual increase through the night
54 until the next morning, whereas CH₄ and CO at Chanban did not show any noticeable diurnal
55 variations.

56 These measurements provide the first insights into diurnal and seasonal variation of key
57 greenhouse gases and air pollutants and their local and regional sources, which are important
58 information for the atmospheric research in the region.

59 **1 Introduction**

60 The average atmospheric mixing ratios of two major greenhouse gases (GHGs), CO₂ and CH₄,
61 have increased by about 40% (from 278 to 390.5 ppm) and about 150% (from 722 to 1803 ppb)
62 respectively since pre-industrial times (~1750 AD). This is mostly attributed to anthropogenic
63 emissions (IPCC, 2013). The current global annual rate of increase of the atmospheric CO₂
64 mixing ratio is 1-3 ppm, with average annual mixing ratios now exceeding a value of 400 ppm at
65 the background reference location in Mauna Loa (WMO, 2016). Between 1750 and 2011,
66 240(±10) PgC of anthropogenic CO₂ was accumulated in the atmosphere of which two thirds
67 were contributed by fossil fuel combustion and cement production, with the remaining coming
68 from deforestation and land use/land cover changes (IPCC, 2013). CH₄ is the second largest
69 gaseous contributor to anthropogenic radiative forcing after CO₂ (Forster et al., 2007). The major
70 anthropogenic sources of atmospheric CH₄ are rice paddies, ruminants and fossil fuel use,
71 contributing approximately 60% to the global CH₄ budget (Chen and Prinn, 2006; Schneising et
72 al., 2009). The remaining fraction is contributed by biogenic sources such as wetlands and
73 fermentation of organic matter by microbes in anaerobic conditions (Conrad, 1996).

74 Increasing atmospheric mixing ratios of CO₂ and CH₄ and other GHGs and short-lived climate-
75 forcing pollutants (SLCPs) such as black carbon (BC) and tropospheric ozone (O₃) have caused
76 the global mean surface temperature to increase by 0.85°C from 1880 to 2012. The surface
77 temperature is expected to increase further by up to 2 degrees at the end of the 21st century in
78 most representative concentration pathways (RCP) emission scenarios (IPCC, 2013). The
79 increase in surface temperature is linked to melting of glaciers and ice sheets, sea level rise,
80 extreme weather events, loss of biodiversity, reduced crop productivity, and economic losses
81 (Fowler and Hennessy, 1995; Guoxin and Shibasaki, 2003).

82 Seventy percent of global anthropogenic CO₂ is emitted in urban areas (Fragkias et al., 2013).
83 Developing countries may have lower per capita GHG emissions than developed countries, but

84 the large cities in developing countries, with their high population and industrial densities, are
85 major consumers of fossil fuels and thus, emitters of GHGs. South Asia, a highly populated
86 region with rapid growth in urbanization, motorization, and industrialization in recent decades,
87 has an ever increasing fossil fuel demand and its combustion emitted 444 Tg C/year in 2000
88 (Patra, et al., 2013), or about 5% of the global total CO₂ emissions. Furthermore, a major
89 segment of the population in South Asia has an agrarian economy and uses biofuel for cooking
90 activities, and agro-residue burning is also common practice in the region, which are important
91 major sources of air pollutants and greenhouse gases in the region (CBS, 2011; Pandey et al.,
92 2014; Sinha et al., 2014).

93 The emission and uptake of CO₂ and CH₄ follow a distinct cycle in South Asia. By using inverse
94 modeling, Patra et al. (2011) found a net CO₂ uptake (0.37 ± 0.20 Pg C yr⁻¹) during 2008 in
95 South Asia and the uptake (sink) is highest during July-September. The remaining months act as
96 a weak gross sink but a moderate gross source for CO₂ in the region. The observed variation is
97 linked with the growing seasons. Agriculture is a major contributor of methane emission. For
98 instance, in India it contributes to 75% of CH₄ emissions (MoEF, 2007). Ambient CH₄
99 concentrations are highest during June to September (peaking in September) in South Asia which
100 are also the growing months for rice paddies (Goroshi et al., 2011). The minimum column
101 averaged CH₄ mixing ratios are in February-March (Prasad et al., 2014).

102 Climate change has impacted South Asia in several ways, as evident in temperature increase,
103 change in precipitation patterns, higher incidence of extreme weather events (floods, droughts,
104 heat waves, cold waves), melting of snowfields and glaciers in the mountain regions, and
105 impacts on ecosystems and livelihoods (ICIMOD, 2009; MoE, 2011). Countries such as Nepal
106 are vulnerable to impacts of climate change due to inadequate preparedness for adaptation to
107 impacts of climate change (MoE, 2011). Decarbonization of its economy can be an important
108 policy measure in mitigating climate change. Kathmandu Valley is one of the largest
109 metropolitan cities in the foothills of the Hindu Kush-Himalaya which has significant reliance on
110 fossil fuels and biofuels. In 2005, fossil fuel burning accounted for 53% of total energy
111 consumption in the Kathmandu Valley, while biomass and hydroelectricity were 38% and 9%,
112 respectively (Shrestha and Rajbhandari, 2010). Fossil fuel consumed in the Kathmandu Valley

113 accounts for 32% of the country's fossil fuel imports, and the major fossil fuel consumers are
114 residential (53.17%), transport (20.80%), industrial (16.84%), and commercial (9.11%) sectors.
115 Combustion of these fuels in traditional technologies such as Fixed Chimney Bulls Trench Kiln
116 (FCBTK) and low efficiency engines (vehicles, captive power generator sets etc.) emit
117 significant amounts of greenhouse gases and air pollutants. This has contributed to elevated
118 ambient concentrations of particulate matter (PM), including black carbon and organic carbon,
119 and several gaseous species such as ozone, polycyclic aromatic hydrocarbons (PAHs),
120 acetonitrile, benzene and isocyanic acid (Pudasainee et al., 2006; Aryal et al., 2009; Panday and
121 Prinn, 2009; Sharma et al., 2012; World Bank, 2014; Chen et al., 2015; Putero et al., 2015;
122 Sarkar et al., 2016). The ambient levels often exceed national air quality guidelines (Pudasainee
123 et al., 2006; Aryal et al., 2009; Putero et al., 2015) and are comparable or higher than ambient
124 levels observed in other major cities in South Asia.

125 Past studies in the Kathmandu Valley have focused mainly on a few aerosols species (BC, PM)
126 and short-lived gaseous pollutants such as ozone and carbon monoxide (Pudasainee et al., 2006;
127 Aryal et al., 2009; Panday and Prinn, 2009; Sharma et al., 2012, Putero et al., 2015). To the best
128 of authors' knowledge, no direct measurements of CO₂ and CH₄ are available for the Kathmandu
129 Valley. Recently, emission estimates of CO₂ and CH₄ were derived for the Kathmandu Valley
130 using the International Vehicle Emission (IVE) model (Shrestha et al., 2013). The study
131 estimated 1554 Gg of annual emission of CO₂ from a fleet of vehicles (that consisted of public
132 buses, 3-wheelers, taxis and motor cycles; private cars, trucks and non-road vehicles were not
133 included in the study) for the year 2010. In addition, the study also estimated 1.261 Gg of CH₄
134 emitted from 3 wheelers (10.6 %), taxis (17.7 %) and motorcycles (71 %) for 2010.

135 This study presents the first 12 months of measurements of two key GHGs, CH₄ and CO₂ along
136 with other trace gases and meteorological parameters in Bode, a semi-urban site in the eastern
137 part of the Kathmandu Valley. The year-long measurement in Bode is a part of the SusKat-ABC
138 (Sustainable Atmosphere for the Kathmandu Valley – Atmospheric Brown Clouds) international
139 air pollution measurement campaign conducted in and around the Kathmandu Valley from
140 December 2012 to June 2013. Details of the SusKat-ABC campaign are described in Rupakheti
141 et al. (2017, manuscript in preparation). The present study provides a detailed account of

142 seasonal and diurnal behaviors of CO₂ and CH₄ and their possible sources. To examine the rural-
143 urban differences and estimate the urban enhancement, these gaseous species were also
144 simultaneously measured for about three months (Jul-Oct) in 2015 at Chanban, a rural site about
145 25 km (aerial distance) outside and southwest of Kathmandu Valley. The seasonality of the trace
146 gases and influence of potential sources in various (wind) directions are further explored by via
147 ratio analysis. This measurement provides unique data from highly polluted but relatively poorly
148 studied region (central Himalayan foothills in South Asia) which could be useful for validation
149 of emissions estimates, model outputs and satellite observations. The study, which provides new
150 insights on potential sources, can also be a good basis for designing mitigation measures for
151 reducing emissions of air pollutants and controlling greenhouse gases in the Kathmandu Valley
152 and the region.

153 **2 Experiment and Methodology**

154 **2.1 Kathmandu Valley**

155 The Kathmandu Valley consists of three administrative districts: Kathmandu, Lalitpur, and
156 Bhaktapur, situated between 27.625° N, 27.75° N and 85.25°E, 85.375°E. It is a nearly circular
157 bowl-shaped valley with a valley floor area of approximately 340 km² located at an altitude of
158 1300 m mean sea level (masl). The surrounding mountains are close to 2000-2800 in height
159 above sea level with five mountain passes located at about 200-600 m above the valley floor and
160 an outlet for the Bagmati River southwest of the Kathmandu Valley. Lack of decentralization in
161 in Nepal has resulted in the concentration of economic activities, health and education facilities,
162 the service sector, as well as most of the central governmental offices in the Kathmandu Valley.
163 Consequently, it is one of the fastest growing metropolitan areas in South Asia with a current
164 population of about 2.5 million, and the population growth rate of 4% per year (World Bank,
165 2013) Likewise, approximately 50% of the total vehicle fleet (2.33 million) of the country is in
166 Kathmandu Valley (DoTM, 2015). The consumption of fossil fuels such as liquefied petroleum
167 gas (LPG), kerosene for cooking and heating dominates the residential consumption, while the
168 rest use biofuel (fuelwood, agro-residue, animal dung) for cooking and heating in the Kathmandu
169 Valley. The commercial sector is also growing in the valley, and the latest data indicate the

170 presence of 633 industries of various sizes. These are mainly associated with dyeing, brick kilns,
171 and manufacturing industries. Fossil fuels such as coal and biofuels are the major fuels used in
172 brick kilns. Brick kilns are reported as one of the major contributors of air pollution in the
173 Kathmandu Valley (Chen et al., 2015; Kim et al., 2015; Sarkar et al., 2016). There are about 115
174 brick industries in the valley (personal communication with M. Chitrakar, President of the
175 Federation of Nepalese Brick Industries). Acute power shortage in the Valley is common all
176 around the year, especially in the dry season (winter/pre-monsoon) when the power cuts can last
177 up to 12 hours a day (NEA, 2014). Energy demand during the power cut period is met with the
178 use of small (67% of 776 generators surveyed for the World Bank study was with capacity less
179 than 50kVA) but numerous captive power generators (diesel/petrol), which further contribute to
180 valley's poor air quality. According to the World Bank's estimate, over 250,000 such generator
181 sets are used in the Kathmandu Valley alone, producing nearly 200 MW of captive power, and
182 providing about 28% of the total electricity consumption of the valley (World Bank, 2014).
183 Apart from these sources, trash burning, which is a common practice (more prevalent in winter)
184 throughout the valley, is one of the major sources of air pollutants and GHGs.

185 Climatologically, Kathmandu Valley has a sub-tropical climate with annual mean temperature of
186 18°C, and annual average rainfall of 1400 mm, of which 90% occurs in monsoon season (June-
187 September). The rest of the year is dry with some sporadic rain events. The wind circulation at
188 large scale in the region is governed by the Asian monsoon circulation and hence the seasons are
189 also classified based on such large scale circulations and precipitation: Pre-Monsoon (March-
190 May), Monsoon (June-September), Post-Monsoon (October-November) and Winter (December-
191 February). Sharma et al. (2012) used the same classification of seasons while explaining the
192 seasonal variation of BC concentrations observed in the Kathmandu Valley. Locally in the
193 valley, the mountain-valley wind circulations play an important role in influencing air quality.
194 The wind speed at the valley floor is calm ($\leq 1 \text{ m s}^{-1}$) in the morning and night, while a westerly
195 wind develops after 11:00 AM in the morning till dusk, and switches to a mild easterly at night
196 (Panday and Prinn, 2009; Regmi et al., 2003). This is highly conducive to building up of air
197 pollution in the valley, which gets worse during the dry season.

198 **2.2 Study sites**

199 Two sites, a semi-urban site within the Kathmandu Valley and a rural site outside the Kathmandu
200 Valley, were selected for this study. The details of the measurements carried out in these sites is
201 described Table 1 and in section 2.2.1 and 2.2.2.

202 **2.2.1 Bode (SusKat-ABC supersite)**

203 The SusKat-ABC supersite was set up at Bode, a semi-urban location (Figure 1) of the
204 Madhyapur Thimi municipality in the Bhaktapur district in the eastern side of the Kathmandu
205 Valley. The site is located at 27.68⁰N latitude, 85.38⁰E longitude, and 1344 masl. The local area
206 around the site has a number of scattered houses and agricultural fields. The agriculture fields are
207 used for growing rice paddies in the monsoon season. It also receives outflow of polluted air
208 from three major cities in the valley: Kathmandu Metropolitan City and Lalitpur Sub-
209 metropolitan City, both mainly during daytime, and Bhaktapur Sub-metropolitan City mainly
210 during nighttime. Among other local sources around the site, about 10 brick kilns are located in
211 the east and southeast direction, approximately within 1-4 km from the site which are operational
212 only during dry season (January to April). There are close to 20 small and medium industries
213 (pharmaceuticals, plastics, electronics, tin, wood, aluminum, iron, and fabrics etc.) scattered in
214 the same direction. The Tribhuvan International Airport (TIA) is located approximately 4 km
215 away to the west of the Bode site.

216 **2.2.2 Chanban**

217 Chanban is a rural/background site in Makwanpur district outside of the Kathmandu Valley
218 (Figure 1). This site is located ~25 km aerial distance due southwest from Bode. The site is
219 located on a small ridge (27.65⁰N, 85.14⁰E, 1896 masl) between two villages - Chitlang and
220 Bajrabarahi - within the forested watershed area of Kulekhani Reservoir, which is located ~ 4.5
221 km southwest of the site. The instruments were set up on the roof of 1-storey building in an open
222 space inside the Nepali Army barrack. There was a kitchen of the army barrack at about 100 m to
223 the southeast of the measurement site. The kitchen uses LPG, electricity, kerosene, and firewood
224 for cooking activities.

225 **2.3 Instrumentation**

226 The measurements were carried out in two phases in 2013-2014 and 2015. In phase one, a cavity
227 ring down spectrometer (Picarro G2401, USA) was deployed in Bode to measure ambient CO₂,
228 CH₄, CO, and water vapor mixing ratios. Twelve months (6 March 2013 - 5 March 2014) of
229 continuous measurements were made in Bode. The operational details of the instruments
230 deployed in Bode are also provided in Table 1. In phase two, simultaneous measurements were
231 made in Bode and Chanban for a little less than 3 months (15 July to 03 October 2015).

232 The Picarro G2401 analyzer quantifies spectral features of gas phase molecules by using a novel
233 wavelength-scanned cavity ring down spectroscopic technique (CRDS). The instrument has a 30
234 km path length in a compact cavity that results high precision and sensitivity. Because of the
235 high precision wavelength monitor, it uses absolute spectral position and maintains accurate peak
236 quantification. Further, it only monitors the special features of interest for reducing the drift. The
237 instrument also has water correction to report dry gas fraction. The reported measurement
238 precision for CO₂, CH₄, CO and water vapor in dry gas is < 150 ppb, < 30 ppb, < 1ppb and < 200
239 ppm for 5 seconds with 1 standard deviation (Picarro, 2015).

240 In Bode, the Picarro analyzer was placed on the 4th floor of a 5-storey building with an inlet at
241 0.5 m above the roof of the building with a 360 degree view (total inlet height: 20 m above
242 ground). The sample air was filtered at the inlet to keep dust and insects out and was drawn into
243 the instrument through a 9 m Teflon tube (1/4 inches ID). The Picarro analyzer was set to record
244 data in every 5 second and recorded both directly sampled data and water corrected data of CO₂
245 and CH₄. In this paper, only water-corrected or dry mixing ratios of CH₄ and CO₂ were used to
246 calculate the hourly averages for diurnal and seasonal analysis.

247 The instruments were factory calibrated before commencing the field measurement. Picarro
248 G2401 model is designed for remote application and long term deployment with minimal drift
249 and less requirement for intensive calibration (Crosson, 2008) and thus was chosen for the
250 current study in places like Kathmandu where there is no or limited availability of high quality
251 reference gases. Regular calibration of Picarro G2401 in field during 2013-2014 deployment was
252 not conducted due to challenges associated with the quality of the reference gas, especially for
253 CO and CH₄. One time calibration was performed for CO₂ (at 395, and 895 ppmv) in July 2015

254 before commencing the simultaneous measurement in Bode and Chanban in 2015. The
255 difference between CO₂ mixing ratio reported by the analyzer and reference mixing ratio was
256 within 5%. CO observations from Picarro G2401 were compared with observations from another
257 CO analyzer (Horiba, model AP370) that was also operated in Bode for 3 months (March - May
258 2013). Horiba CO monitor was a new unit, which was factory calibrated before its first
259 deployment in Bode. Nevertheless, this instrument was inter-compared with another CO analyzer
260 (same model) from the same manufacturer prior to the campaign and its correlation coefficient
261 was 0.9 [slope of data from the new unit (y-axis) vs the old unit (x-axis) = 1.09]. Primary gas
262 cylinders from Linde UK (1150 ppbv) and secondary gases from Ultra-Pure Gases and
263 Chemotron Science Laboratories (1790 ppbv) were used for the calibration of CO instrument.
264 Further details on CO measurements and calibration of Horiba AP370 can be found in Sarangi et
265 al. (2014; 2016). Statistically significant correlation ($r = 0.99$, slope = 0.96) was found between
266 Picarro and Horiba hourly average CO mixing ratio data (Supplementary Information Figure S1).
267 Furthermore, the monthly mean difference between these two instruments (Horiba AP370 minus
268 Picarro G2401) was calculated to be 0.02 ppm (3%), 0.04 ppm (5%) and 0.02 ppm (4%) in
269 March, April and May, respectively. For the comparison period of 3 months, the mean difference
270 was 0.02 ppm (4%). Overall differences were small to negligible during the comparison period
271 and thus, adjustment in the data was deemed not necessary.

272 Besides highly selective to individual species, Picarro G2401 has a water correction function and
273 thus accounts for the any likely drift in CO, CO₂ and CH₄ mixing ratios with the fluctuating
274 water vapor concentration (Chen et al., 2013; Crosson, 2008). Crosson (2008) also estimated a
275 peak to peak drift of 0.25 ppmv. Further, Crosson (2008) observed a 1.2 ppbv/day drift in CO₂
276 after 170 days from the initial calibration. For a duration of one year the drift will be less than 1
277 ppmv, which is less than 1% of the observed mixing ratio in (hourly ranges: 376-537 ppm) Bode
278 even if the drift was in same magnitude as in case of Crosson (2008). Crosson (2008) reported
279 0.8 ppbv peak to peak drift in CH₄ measurements for 18 days after the initial calibration.

280 There were other instruments concurrently operated in Bode; a ceilometer for measuring mixing
281 layer height (Vaisala Ceilometer CL31, Finland), and an Automatic Weather Station (AWS)
282 (Campbell Scientific, USA). The ceilometer was installed on the rooftop (20 m above ground) of

283 the building (Mues et al., 2017). For measuring the meteorological parameters, a Campbell
284 Scientific AWS (USA) was set up on the roof of the building with sensors mounted at 2.9 m
285 above the surface of the roof (22.9 m from the ground). The Campbell Scientific AWS measured
286 wind speed and direction, temperature, relative humidity and solar radiation every minute.
287 Temperature and rainfall data were taken from an AWS operated by the Department of
288 Hydrology and Meteorology (DHM), Nepal at the Tribhuvan International Airport (TIA, see
289 Figure 1), ~4 km due west of Bode site.

290 At Chanban, the inlet for Picarro gas analyzer was kept on the rooftop ~3 m above the ground
291 and the sample air was drawn through a 3 m long Teflon tube (1/4 inches ID). The sample was
292 filtered at the inlet with a filter (5-6 μm pore size) to prevent aerosol particles from getting into
293 the analyzer. An automatic weather station (Davis Vantage Pro2, USA) was also set up in an
294 open area, about 17 m away from the building and with the sensors mounted at 2 m above
295 ground.

296 **3. Results and discussion**

297 The results and discussions are organized as follow: Sub-section 3.1 describes a year round
298 variation in CH_4 , CO_2 , CO and water vapor at Bode; sub-sections 3.2, 3.3 present the analysis of
299 the observed monthly and seasonal variations and diurnal variation. Sub-sections 3.4 and 3.5
300 about the interrelation of CO_2 , CH_4 and CO and potential emission sources in the valley and sub-
301 section 3.6 compares and contrasts CH_4 , CO_2 , CO at Bode and Chanban.

302 **3.1 Time series of CH_4 , CO_2 , CO and water vapor mixing ratios**

303 Figure 2 shows the time series of hourly mixing ratios of CH_4 , CO_2 , CO, and water vapor at
304 Bode. Meteorological data from Bode and the Tribhuvan International Airport are also shown in
305 Figure 2. Data gaps in Figure 2a and 2b were due to maintenance of the measurement station. In
306 general, the changes observed in CO mixing ratio was higher in terms of % change than the
307 variations observed in CH_4 and CO_2 mixing ratios during the sampling period. In contrast, CO
308 mixing ratios decreased and water vapor mixing ratios increased significantly during the rainy
309 season (June-September). For the entire sampling period, the annual average (\pm one standard

310 deviation) of CH₄, CO₂, CO, and water vapor mixing ratios were 2.192 (± 0.066) ppm, 419.3
311 (± 6.0) ppm, 0.50 (± 0.23) ppm, and 1.73 (± 0.66)%, respectively. The relative variabilities for the
312 annual average of CH₄, CO₂ and CO were thus 3%, 1.4% and 46%, respectively. Their
313 variabilities at Mauna Loa were CH₄: 6% and CO₂: 0.5% and at Waliguan were CH₄: 0.48%,
314 CO₂: 0.9%. The high variability in the annual mean, notably for CO in Bode could be indicative
315 of the seasonality of emission sources and meteorology. The annual CH₄ and CO₂ mixing ratios
316 were compared to the historical background site (Mauna Loa Observatory, Hawaii, USA) and the
317 background site (Waliguan, China) in Asia, which will provide insight on spatial differences.
318 The selection of neighboring Indian urban and semi-urban sites, where many emission sources
319 are typical for the region, for comparison provides information on relative differences
320 (higher/lower), which will help in investigating possible local emission sources in the valley. As
321 expected, annual mean of CH₄ and CO₂ mixing ratios in the Kathmandu Valley were higher than
322 the levels observed at background sites in the region and elsewhere (Table 4). We performed a
323 significance test at 95% confidence level (t-test) of the annual mean values between the sites to
324 evaluate whether the observed difference is statistically significant ($p < 0.05$), which was
325 confirmed for the annual mean CH₄ and CO₂ between Bode and Mauna Loa, and between Bode
326 and Waliguan. CH₄ was nearly 20% higher at Bode than at Mauna Loa observatory ($1.831 \pm$
327 0.110 ppm) (Dlugokencky et al., 2017) and ca.17% higher than at Mt. Waliguan (1.879 ± 0.009
328 ppm) for the same observation period (Dlugokencky et al., 2016). The slightly higher CH₄
329 mixing ratios between at Bode and Waliguan than at Mauna Loa Observatory could be due to
330 rice farming as a key source of CH₄ in this part of Asia. Thus, it could be associated with such
331 agricultural activities in this region. Similarly, the annual average CH₄ at Bode during 2013-14
332 was found comparable to an urban site in Ahmedabad (1.880 ± 0.4 ppm, i.e., variability: 21.3%)
333 in India for 2002 (Sahu and Lal, 2006) and 14% higher than in Shadnagar (1.92 ± 0.07 ppm, i.e.,
334 variability: 3.6%), a semi-urban site in Telangana state (~70 km north from Hyderabad city)
335 during 2014 (Sreenivas et al., 2016). Likewise, the difference between annual mean mixing
336 ratios at Bode (419.3 ± 6.0 ppm, 1.4% variability) vs. Mauna Loa (396.8 ± 2.0 ppm, 0.5%
337 variability) (NOAA, 2015) and Bode vs. Waliguan (397.7 ± 3.6 ppm, 0.9% variability)
338 (Dlugokencky et al., 2016a) is statistically significant ($p < 0.05$).

339

340 The high CH₄ and CO₂ mixing ratios at Bode in comparison to Ahmedabad and Shadnagar could
341 be due to more than 115 coal-biomass fired brick kiln, some of them are located near the site
342 (less than 4 km) and confinement of pollutants within the Valley due to bowl shaped topography
343 of the Kathmandu Valley. Although Ahmedabad is a big city with high population larger than
344 Kathmandu Valley but the measurement site is far from the nearby heavy polluting industries
345 and situated in plains, where ventilation of pollutants would be more efficient as opposed to the
346 Kathmandu Valley. The major polluting sources were industries, residential cooking and
347 transport sector in Ahmedabad (Chandra et al., 2016). Shadnagar is a small town with a
348 population of 0.16 million and major sources were industries (small-medium), biomass burning
349 in residential cooking (Sreenivas et al., 2016).

350 The monthly average of CO₂ mixing ratios in 2015 in Chanban (Aug: 403.4, Sep: 399.1 ppm)
351 were slightly higher than the background sites at Mauna Loa Observatory (Aug: 398.89 ppm,
352 Sep: 397.63 ppm) (NOAA, 2015) and Mt. Waliguan (Aug: 394.55 ppm, Sep: 397.68 ppm)
353 (Dlugokencky et al., 2016a). For these two months in 2015, CH₄ mixing ratios were also higher
354 in Bode (Aug: 2.281ppm, Sep: 2.371 ppm) and Chanban (Aug: 2.050 ppm, Sep: 2.102 ppm)
355 compared to Mauna Loa Observatory (Aug: 1.831 ppm, Sep: 1.846 ppm) (Dlugokencky et al.,
356 2017)) and Mt. Waliguan (Aug: 1.915 ppm, 1.911 ppm) (Dlugokencky et al., 2016). The low
357 differences in CO₂ between Chanban and background sites mentioned above indicate the less
358 number of and/or less intense CO₂ sources at Chanban during these months because of the lack
359 of burning activities due to rainfall in the region. The garbage and agro-residue burning activities
360 were also absent or reduced around Bode during the monsoon period. However, high CH₄ values
361 in August and September in Bode, Chanban and Mt. Waliguan in comparison to Mauna Loa
362 Observatory may indicate the influence of CH₄ emission from paddy fields in the Asian region.

363 **3.2 Monthly and Seasonal variations**

364 Figure 3 shows the monthly box plot of hourly CH₄, CO₂, CO and water vapor observed for a
365 year in Bode. Monthly and seasonal averages of CH₄ and CO₂ mixing ratios at Bode are
366 summarized in Table 2 and 3. CH₄ were lowest during May-July (ranges from 2.093-2.129 ppm)
367 period and highest during August-September (2.274-2.301 ppm), followed by winter. In addition

368 to the influence of active local sources, the shallow boundary layer in winter was linked to
369 elevated concentrations (Panday and Prinn, 2009; Putero et al., 2015, Mues et al., 2017). The low
370 CH₄ values from May to July may be associated with the absence of brick kiln and frequent
371 rainfall in these months. Brick kiln were operational during January to April. Rainfall also leads
372 to suppression of open burning activities in the valley (see Figure 2b). The CH₄ was slightly
373 higher (statistically significant, $p < 0.05$) in monsoon season (July –September) than pre-monsoon
374 season (unlike CO₂ which was higher in pre-monsoon), and could be associated with the addition
375 of CH₄ flux from the water-logged rice paddies (Goroshi et al., 2011). There was a visible drop
376 in CH₄ from September to October but remained consistently over 2.183 ppm from October to
377 April with little variation between these months. Rice-growing activities are minimal or none in
378 October and beyond, and thus may be related to the observed dip in CH₄ mixing ratio.

379 Comparison of seasonal average CH₄ mixing ratios at Bode and Shadnagar (a semi-urban site in
380 India) indicated that CH₄ mixing ratios at Bode were higher in all seasons than at Shadnagar:
381 pre-monsoon (1.89 ± 0.05 ppm), monsoon (1.85 ± 0.03 ppm), post-monsoon (2.02 ± 0.01 ppm),
382 and winter (1.93 ± 0.05 ppm) (Sreenivas et al., 2016). The possible reason for lower CH₄ at
383 Shadnagar in all season could be associated with geographical location and difference in local
384 emission sources. The highest CH₄ mixing ratio in Shadnagar was reported in post-monsoon
385 which was associated with harvesting in the Kharif season (July – October), while the minimum
386 was in monsoon. Shadnagar is a relatively small city (population: ~0.16 million) compared to
387 Kathmandu Valley and the major local sources which may have influence on CH₄ emission
388 include bio-fuel, agro-residue burning and residential cooking.

389 The seasonal variation in CO₂ could be due to (i) the seasonality of major emission sources such
390 as brick, (ii) seasonal growth of vegetation (CO₂ sink) (Patra et al., 2011) and (iii) atmospheric
391 transport associated with regional synoptic atmospheric circulation (monsoon circulation and
392 westerly disturbance in spring season) which could transport regional emission sources from
393 vegetation fire and agriculture residue burning (Putero et al., 2015), and a local mountain-valley
394 circulation effect (Kitada and Regmi, 2003; Panday et al., 2009). The concentrations of most
395 pollutants in the region are lower during the monsoon period (Sharma et al., 2012, Marinoni,
396 2013; Putero et al., 2015) because frequent and heavy rainfall suppresses emission. We saw a

397 drop in the CO₂ mixing ratio during the rainfall period due to changes in various processes such
398 as enhanced vertical mixing, uptake of CO₂ by vegetation and soils, and where relevant reduction
399 in combustion sources. CO₂ can also dissolve into rainfall, forming carbonic acid, which may
400 lead to a small decrease in the CO₂ mixing ratio as has been observed during heavy intensity
401 rainfall (Mahesh et al., 2014; Chaudhari et al., 2007). Monsoon is also the growing season with
402 higher CO₂ assimilation by plants than other seasons (Sreenivas et al., 2016). In contrast, winter,
403 pre-monsoon and post-monsoon season experiences an increase in emission activities in the
404 Kathmandu Valley (Putero et al., 2015).

405
406 The CO₂ mixing ratios were in the range of 376 - 537 ppm for the entire observation period.
407 Differences with CH₄ were observed in September and October where CO₂ was increasing
408 (mean/median) in contrast to CH₄ which showed the opposite trend. The observed increase in
409 CO₂ after October may be related to less or no rainfall, which results in the absence of rain-
410 washout and/or no suppression of active emission sources such as open burning activities.
411 However, the reduction in CH₄ after October could be due to reduced CH₄ emissions from paddy
412 fields, which were high in August-September. CO₂ remains relatively lower during July-August,
413 but it is over 420 ppm from January to May. Seasonal variation of CO₂ in Bode was similar in
414 seasonal variation but the values are higher than the values observed in Shadnagar, India
415 (Sreenivas et al., 2016).

416 The variations in CO were more distinct than CH₄ and CO₂ during the observation period
417 (Figure 3). The highest CO values were observed from January-April (0.71-0.91 ppm). The
418 seasonal mean of CO mixing ratios at Bode were: pre-monsoon (0.60 ±0.36 ppm), monsoon
419 (0.26±0.09 ppm), post-monsoon (0.40±0.15 ppm), and winter (0.76±0.43 ppm). The maximum
420 CO was observed in winter, unlike CO₂ which was maximum in pre-monsoon. The high CO in
421 winter was due to the presence of strong local pollution sources (Putero et al., 2015) and shallow
422 mixing layer heights. The addition of regional forest-fire and agro-residue burning augmented
423 CO₂ mixing ratios in pre-monsoon. The water vapor mixing ratio showed a seasonal pattern
424 opposite of CO, with a maximum in monsoon (2.53 %) and minimum in winter (0.95 %), and
425 intermediate values of 1.56 % in pre-monsoon and 1.55 % in post-monsoon season.

426 There were days in August-September when the CH₄ increases by more than 3 ppm (Figure 2).
427 Enhancement in CO₂ was also observed during the same time period. In the absence of tracer
428 model simulations, the directionality of the advected air masses is unclear. Figure 4 shows that
429 during these two months, CO₂ mixing ratios were particularly high (> 450 CO₂ and > 2.5 ppm
430 CH₄) with the air masses coming from the Northeast-East (NE-E). CO during the same period
431 was not enhanced and didn't show any particular directionality compared to CH₄ and CO₂
432 (Figure 4c). Areas NE-E to Bode are predominantly irrigated (rice paddies) during August-
433 September, and sources such as brick kilns were not operational during this time period. Goroshi
434 et al. (2011) reported that June to September is a growing season for rice paddies in South Asia
435 with high CH₄ emissions during these months and observed a peak in September in the
436 atmospheric CH₄ column over India. Model analysis also points to high methane emissions in
437 September which coincides with the growing period of rice paddies (Goroshi et al., 2011, Prasad
438 et al., 2014). The CH₄ mixing ratios at Bode in January (2.233 ± 0.219 ppm) and July ($2.129 \pm$
439 0.168 ppm) were slightly higher than the observation in Darjeeling (Jan: 1.929 ± 0.056 ppm; Jul:
440 1.924 ± 0.065 ppm), a hill station of eastern Himalaya (Ganesan et al., 2013). The higher CH₄
441 values in January and July at Bode compared to Darjeeling could be because of the influence of
442 local sources, in addition to the shallow boundary layer in Kathmandu Valley. Trash burning and
443 brick kilns are two major sources from December until April in the Kathmandu Valley while
444 emission from paddy fields occurs during July-September in the Kathmandu Valley. In contrast,
445 the measurement site in Darjeeling was located at higher altitude (2194 masl) and was less
446 influenced by the local emission. The measurement in Darjeeling reflected a regional
447 contribution. There are limited local source in Darjeeling such as wood biomass burning, natural
448 gas related emission and vehicular emission (Ganesan et al., 2013).

449 The period between January and April had generally higher or the highest values of CO₂, CH₄
450 and CO at Bode. The measurement site was impacted mainly by local Westerly-Southwesterly
451 winds (W-SW) and East-Southeast (E-SE). The W-SW typically has a wind speed in the range
452 $\sim 1 - 6 \text{ m s}^{-1}$ and was active during late morning to afternoon period ($\sim 11:00$ to $17:00$ NST,
453 supplementary information Figure S2 and S3). Major cities in the valley such as Kathmandu
454 Metropolitan City and Lalitpur Sub-metropolitan City are W-SW of Bode (Figure 1c). Wind

455 from E-SE were generally calm ($\leq 1 \text{ m s}^{-1}$) and observed only during night and early morning
456 hours (21:00 to 8:00 NST). The mixing ratio of all three species in air mass from the E-SE was
457 significantly higher than in the air mass from W-SW (Figure 4). There are 10 biomass co-fired
458 brick kilns and Bhaktapur Industrial Estate located within 1-4 km E-SE from Bode (Sarkar et al.,
459 2016). The brick kilns were only operational during January-April. Moreover, there were over
460 100 brick kilns operational in the Kathmandu Valley (Putero et al., 2015) which use low-grade
461 lignite coal imported from India and biomass fuel to fire bricks in inefficient kilns (Brun, 2013).

462 Fresh emissions from main city center were transported to Bode during daytime by W-SW winds
463 which mainly include vehicular emission. Compared to monsoon months (June-August), air
464 mass from W-SW had higher values in all three species (Figure 4) during winter and pre-
465 monsoon months. This may imply that in addition to vehicular emission, there are other potential
466 sources which were exclusively active during these dry months. Municipal trash burning is also
467 common in the Kathmandu Valley, with a reported higher frequency from December to February
468 (Putero et al., 2015). The frequency in the use of captive power generator sets are highest during
469 the same period, which is another potential source contributing to air coming from W-SW
470 direction (World Bank, 2014; Putero et al., 2015).

471 Regional transport of pollutants into the Kathmandu Valley was reported by Putero et al. (2015).
472 To relate the influence of synoptic circulation with the observed variability in BC and O₃ in the
473 Kathmandu Valley, 5-day back trajectories (of air masses arriving in the Kathmandu Valley)
474 were computed by Putero et al., (2015) using the HYSPLIT model. These individual trajectories
475 which were initialized at 600 hPa, for the study period of one year and were clustered into nine
476 clusters. Of the identified clusters, the most frequently observed clusters during the study period
477 were the Regional and Westerly cluster or circulation (22% and 21%). The trajectories in the
478 regional cluster originate within $10^\circ \times 10^\circ$ around the Kathmandu Valley, whereas the majority of
479 trajectories in this westerly cluster originated broadly around $20\text{-}40^\circ \text{ N}$, $\sim 60^\circ \text{ E}$. Putero et al
480 (2015) found that the regional and westerly synoptic circulation were favorable for high values
481 of BC and O₃ in the Kathmandu Valley. Other sources of CO₂ and CH₄ could be due to
482 vegetation fires which were also reported in the region surrounding the Kathmandu Valley
483 during the pre-monsoon months (Putero et al., 2015). Similarly, high pollution events, peaking in

484 the pre-monsoon, were observed at Nepal Climate Observatory-Pyramid (NCO-P) near Mt.
485 Everest, which have been associated with vegetation fires in the Himalayan foothills and
486 northern IGP region (Putero et al., 2014). MODIS derived forest counts (Figure 5), which also
487 indicated high frequency of forest fire and farm fire from February to April and also during post-
488 monsoon season. It is interesting that the monthly mean CO₂ mixing ratio was maximum in April
489 (430 ± 27 ppm) which could be linked to the fire events. It is likely that the westerly winds
490 ($>2.5-4.5$ m s⁻¹) during the daytime (supplementary information Figure S2, S3) bring additional
491 CO₂ from vegetation fires and agro-residue burning in southern plains of Nepal including the
492 IGP region (Figure 5). Low values of CO₂ and CH₄ during June-July (Figure 3) was coincident
493 with the rainy season, and sources such as brick kiln emission, trash burning, captive power
494 generators, and regional agriculture residue burning and forest fires are weak or absent during
495 these months.

496 **3.3 Diurnal Variation**

497 Figure 6 shows the average seasonal diurnal patterns of CH₄, CO₂, CO, and water vapor mixing
498 ratios observed at Bode for four seasons. All the three gas species had a distinct diurnal pattern in
499 all seasons, characterized by maximum values in the morning hours (peaked around 7:00-9:00),
500 afternoon minima around 15:00-16:00, and a gradual increase through the evening until next
501 morning. There was no clear evening peak in CH₄ and CO₂ mixing ratios whereas CO shows an
502 evening peak around 20:00. The gradual increase of CO₂ and CH₄ in the evening in contrast to
503 the increase until evening peak traffic hours and later decay of CO may be indicative of a few
504 factors. As pointed out earlier, after the peak traffic hours, there are no particularly strong
505 sources of CO, especially in the monsoon and post-monsoon season. It is also likely that some of
506 the CO is decay due to nighttime katabatic winds which replace polluted air masses with cold
507 and fresh air from the nearby mountain (Panday and Prinn, 2009). As for the CO₂, the biosphere
508 respiration at night in the absence of photosynthesis can add additional CO₂ to the atmosphere
509 which especially in the very shallow nocturnal boundary layer may explains part of the increase
510 of the CO₂ mixing ratio. The well-defined morning and evening peaks observed in CO mixing
511 ratios are associated with the peaks in traffic and residential activities. The CH₄ and CO₂ showed
512 pronounced peaks in the morning hours (07:00-09:00) in all seasons with almost the same level

513 of seasonal average mixing ratios. CO had a prominent morning peak in winter and pre-monsoon
514 season, but the peak was significantly lower in monsoon and post-monsoon. The CO (~1-1.4
515 ppm) around 08:00-09:00 am in winter and pre-monsoon were nearly 3-4 times higher than in
516 monsoon and post-monsoon season. It appears that CH₄ and CO₂ mixing ratios were
517 continuously building up at night until the following morning peak in all seasons. The similar
518 seasonal variations in CH₄ and CO₂ across all seasons could be due to their long-lived nature, as
519 compared to CO, whose diurnal variations are strongly controlled by the evolution of the
520 boundary layer. Kumar et al. (2015) also reported morning and evening peaks and an afternoon
521 low in CO₂ mixing ratios in industrial, commercial, and residential sites in Chennai in India. The
522 authors also found high early morning CO₂ mixing ratios at all sites and attributed it to the
523 temperature inversion and stable atmospheric condition.

524
525 The daytime low CH₄ and CO₂ mixing ratios were due to (i) elevated mixing layer height in the
526 afternoon (Figure 7), (ii) development of upslope wind circulation in the valley, and (iii)
527 development of westerly and southwesterly winds which blows through the valley during the
528 daytime from around 11 am to 5 pm (supplementary information Figure S2), all of which aid in
529 dilution and ventilation of the pollutants out of the valley (Regmi et al., 2003; Kitada and Regmi,
530 2003; Panday and Prinn, 2009). In addition, the daytime CO₂ minimum in the summer monsoon
531 is also associated with high photosynthetic activities in the valley as well as in the broader
532 surrounding region. In the nighttime and early morning, the mixing layer height was low (only
533 around 200-300 m in all seasons) and stable boundary layer for almost 17 hours a day. In the
534 daytime it grows up to 800-1200 m for a short time (ca. from 11:00 to 6:00) (Mues et al., 2017).
535 Therefore the emissions from various activities in the evening after 18:00 (cooking and heating,
536 vehicles, trash burning, and bricks factories in the night and morning) were trapped within the
537 collapsing and shallow boundary layer, and hence mixing ratios were high during evening, night
538 and morning hours. Furthermore, plant and soil respiration also increases CO₂ mixing ratio
539 during the night (Chandra et al., 2016). However, Ganesan et al. (2013) found a distinct diurnal
540 cycle of CH₄ mixing ratios with twin peaks in the morning (7:00-9:00), and afternoon (15:00-
541 17:00) and a nighttime low in winter but no significant diurnal cycle in the summer of 2012 in
542 Darjeeling, a hill station (2194 masl) in the eastern Himalaya. The authors described that the

543 morning peaks could be due to the radiative heating of the ground in the morning, which breaks
544 the inversion layer formed during night, and as a result, pollutants are ventilated from the
545 foothills up to the site. The late afternoon peaks match wind direction and wind speed (upslope
546 winds) that could bring pollution from plains to mountains.

547 The diurnal variation of CO is also presented along with CO₂ and CH₄ in Figure 6c. CO is an
548 indicator of primary air pollution. Although CO mixing ratio showed distinct diurnal pattern, it
549 was different from the diurnal patterns of CO₂ and CH₄. CO diurnal variation showed distinct
550 morning and evening peaks, afternoon minima, and a nighttime accumulation or decay.
551 Nighttime accumulation in CO was observed only in winter and pre-monsoon and decay or
552 decrease in monsoon season and post-monsoon season (Figure 7). The lifetime of CO (weeks to
553 months) is very long compared to the ventilation timescales for the valley, so the different
554 diurnal cycles would be due to differences in nighttime emissions. While the biosphere respire
555 at night which may cause a notable increase in CO₂ in the shallow boundary layer, most CO
556 sources (transport sector, residential cooking) except brick kilns remain shut down or less active
557 at night. This also explains why nighttime values of CO drop less in the winter and pre-monsoon
558 than in other seasons. Furthermore, the prominent morning peaks of CO in pre-monsoon and
559 winter compared to other seasons results from nighttime accumulation, additional fresh
560 emissions in the morning and recirculation of the pollutants due to downslope katabatic winds
561 (Pandey and Prinn, 2009; Panday et al., 2009). Pandey and Prinn (2009) observed nighttime
562 accumulation and gradual decay during the winter (January 2005). The measurement site in
563 Pandey and Prinn (2009) was near the urban core of the Kathmandu Valley and had significant
564 influence from the vehicular sources all over the season including the winter season.
565 Measurement in Bode lies in close proximity to the brick kilns which operate 24 hours during the
566 winter and pre-monsoon period. Calm southeasterly winds are observed during the nighttime and
567 early morning (ca.22:00 – 8:00) in pre-monsoon and winter, which transport emissions from
568 brick kiln to the site (Sarkar et al., 2016). Thus the gradual decay in CO was not observed in
569 Bode.

570 The timing of the CO morning peak observed in this study matches with observations by Panday
571 et al. (2009). They also found CO morning peak at 8:00 in October 2004 and at 9:00 in January

572 2005. The difference could be linked to the boundary layer stability. As the sun rises later in
573 winter, the boundary layer stays stable for a longer time in winter keeping mixing ratios higher in
574 morning hours than in other seasons with an earlier sunrise.

575 The morning peaks of CO₂ and CH₄ mixing ratios occurred around 6:00-7:00 local time in the
576 pre-monsoon, monsoon, and post monsoon season, whereas in winter their peaks are delayed by
577 1-2 hours in the morning; CH₄ at 8:00 and CO₂ at 9:00. The CO showed that its morning peak
578 was delayed compared to CO₂ and CH₄ morning peaks by 1-2 hour in pre-monsoon, monsoon
579 and post-monsoon (at 8:00) and in winter (at 9:00). The occurrence of morning peaks in CO₂ and
580 CH₄ 1-2 hours earlier than CO is interesting. This could be due to the long lifetimes and
581 relatively smaller local sources of CH₄ and CO₂, as CO is mainly influenced by emissions from
582 vehicles during rush hour, as well as from biomass and trash burning in the morning hours. Also,
583 CO increases irrespective of change in mixing layer (collapsing or/rising, Figure 7) but CO₂ and
584 CH₄ start decreasing only after the mixing layer height starts to rise. Recently, Chandra et al.
585 (2016) also reported that the CO₂ morning peak occurred earlier than CO in observations in
586 Ahmedabad City India. This was attributed to CO₂ uptake by photosynthetic activities after
587 sunrise but CO kept increasing due to emissions from the rush hour activities.

588 The highest daytime minimum of CO₂ was observed in the pre-monsoon followed by winter
589 (Figure 6b). The higher daytime minimum of CO₂ mixing ratios in the pre-monsoon season than
590 in other seasons, especially winter, is interesting. The local emission sources are similar in pre-
591 monsoon and winter and the boundary layer is higher (in the afternoon) during the pre-monsoon
592 (~1200 meters) than in winter (~900 meters) (Mues et al., 2017). Also, the biospheric activity in
593 the region is reported to be higher in the pre-monsoon (due to high temperature and solar
594 radiation) than winter (Rodda et al., 2016). Among various possible causes, transport of CO₂ rich
595 air from outside the Kathmandu Valley has been hypothesized as a main contributing factor, due
596 to regional vegetation fire combined with westerly mesoscale to synoptic transport Putero et al.
597 (2015). In monsoon and post-monsoon seasons, the minimum CO₂ mixing ratios in the afternoon
598 drops down to 390 ppm, this was close to the values observed at the regional background sites
599 Mauna Loa and Waliguan.

600

601 **3.4 Seasonal interrelation of CO₂, CH₄ and CO**

602 The Pearson's correlation coefficient (r) between CO₂ and CO was strong in winter (0.87),
603 followed by monsoon (0.64), pre-monsoon (0.52) and post-monsoon (0.32). The higher
604 coefficient in winter indicates that common or similar sources for CO₂ and CO and moderate
605 values in pre-monsoon and monsoon indicates the likelihood of different sources. To avoid the
606 influence of strong diurnal variations observed in the valley, daily averages, instead of hourly,
607 were used to calculate the correlation coefficients. The correlation coefficients between daily
608 CH₄ and CO₂ for four seasons are as follows: winter (0.80), post-monsoon (0.74), pre-monsoon
609 (0.70) and monsoon (0.22). A semi-urban measurement study in India also found a strong
610 positive correlation between CO₂ and CH₄ in the pre-monsoon (0.80), monsoon (0.61), post-
611 monsoon (0.72) and winter (0.8) (Sreenivas et al., 2016). It should be noted here that Sreenivas
612 et al., (2006) used hourly average CO₂ and CH₄ mixing ratios. The weak monsoon correlation at
613 Bode, which is in contrast to Sreenivas et al. (2016), may point to the influence of dominant CH₄
614 emission from paddy field during the monsoon season (Goroshi et al., 2011). Daily CH₄ and CO
615 was also weakly correlated in monsoon (0.34) and post-monsoon (0.45). Similar to CH₄ and
616 CO₂, the correlation between CH₄ and CO were moderate to strong in pre-monsoon (0.76) and
617 winter (0.75).

618 Overall, the positive and high correlations between CH₄ and CO mixing ratios and between CH₄
619 and CO₂ in the pre-monsoon and winter indicate common sources, most likely combustion
620 related sources such as vehicular emission, brick kilns, agriculture fire etc., or the same source
621 regions (i.e. their transport due to regional atmospheric transport mechanisms). Weak
622 correlation, between CH₄-CO₂ and between CH₄-CO, during monsoon season indicates sources
623 other than combustion-related may be active, such as agriculture as a key CH₄ source (Goroshi et
624 al., 2013)

625 **3.5 CO and CO₂ ratio: Potential emission sources**

626 The ratio of the ambient mixing ratios of CO and CO₂ was used as an indicator to help
627 discriminate emission sources in the Kathmandu Valley. The ratio was calculated from the
628 excess (dCO and dCO_2) relative to the background values of ambient CO and CO₂ mixing ratios.

629 The excess value was estimated by subtracting the base value which was calculated as the fifth
630 percentile of the hourly data for a day (Chandra et al., 2016).

631 Average emission ratios from the literature are shown in Table 5, and average ratios of
632 dCO/dCO_2 are shown in Table 6, disaggregated into morning hours, evening hours, and seasonal
633 values. It must be stated that due to the large variance in the calculated ratio from this study
634 (Table 6) as well as the likely variation in the estimated ratio presented in Table 5, the
635 interpretation and conclusion about sources should be cautiously drawn and will be indicative.
636 Higher ratios were found in pre-monsoon (12.4) and winter (15.1) season compared to post-
637 monsoon (8.3) and monsoon (7.5). These seasonal differences in the dCO/dCO_2 ratio are
638 depicted in Figure 8, which shows a clear relationship with the wind direction and associated
639 emissions, with the highest values especially for stronger westerly winds. Compared to the other
640 three seasons, the ratio in winter was also relatively high for air masses from the east, likely due
641 to emissions from brick kilns combined with accumulation during more stagnant meteorological
642 conditions (supplementary information Figure S2, S3). In other seasons, emission emanating
643 from the north and east of Bode were characterized by a dCO/dCO_2 ratio below 15. Air masses
644 from the west and south generally have a ratio from 20 to 50 in all but post-monsoon season,
645 where the ratio sometimes exceeds 50. A ratio of 50 or over is normally due to very inefficient
646 combustion sources (Westerdahl et al., 2009; Stockwell et al., 2016), such as agro-residue
647 burning, which is common during the post-monsoon season in the Kathmandu Valley.

648 For interpretability of emission ratio with sources, the ratio was classified into three categories:
649 (i) 0 – 15, (ii) 15 – 45, and (iii) greater than 45. This classification was based on the observed
650 distribution of emission ratio during the study period (Figure 8) and a compilation of observed
651 emission ratios typical for different sources from Nepal and India (see Table 5). An emission
652 ratio below 15 is likely to indicate residential cooking and diesel vehicles, and captive power
653 generation with diesel-powered generator sets (Smith et al., 2000; ARAI, 2008; World Bank,
654 2014). The emission from brick kilns (FCBTK and Clamp kilns, both common in the Kathmandu
655 Valley), and inefficient, older (built before 2000) gasoline cars fall in between 15 - 45 (Weyant
656 et al., 2014, Stockwell et al., 2016; ARAI, 2008). Four-stroke motorbikes and biomass burning
657 activities (mixed garbage, crop-residue and biomass) are one of the least efficient combustion

658 sources, with emission ratios higher than 45 (Westerdahl et al., 2009; Stockwell et al., 2016;
659 ARAI, 2008).

660 Although ratio of CO/CO₂ is a weak indicator of sources and the mean ratio has large variance
661 (See Table 6), the conclusions drawn, from using Figure 8 and the above mentioned
662 classification, are not conclusive. The estimated CO/CO₂ ratio tentatively indicates that the local
663 plume impacting the measurement site (Bode) from the north and east could be residential and/or
664 diesel combustion. The estimated CO/CO₂ ratio of the local plume from the south and west
665 generally falls in the 15-45 range which could indicate emissions from brick kilns and inefficient
666 gasoline vehicles. Very high ratios were also estimated from the south west during the post-
667 monsoon season. Among other possible sources, this may indicate agro-residue open burning.

668 The emission inventory for CO identifies (aggregate for a year) residential, and gasoline related
669 emission from transport sector (Sadavarte et al., 2017, in preparation). The inventory is not yet
670 temporally resolved, so no conclusion can be drawn about the sources with respect to different
671 seasons. From the 1km x1km emission inventory of the Kathmandu Valley for 2011, the
672 estimated sectoral source apportionment of CO is residential (37%), transport sector (40%) and
673 industrial (20%). The largest fraction from the residential sector is cooking (24 %) whereas the
674 majority of transport sector related CO in the Kathmandu Valley is from gasoline vehicles.

675 The dCO/dCO₂ ratio also changes markedly between the morning peak hours (7:00-9:00, except
676 in winter season when the peak occurs during 8:00-9:00) and evening peak hours (19:00-21:00
677 pm) (Table 6). Morning and evening values were lowest (2.2, 8.0) during the monsoon and
678 highest (11.2, 21.6) in the winter season, which points to the different emission characteristics in
679 these two seasons. This feature is similar to Ahmedabad, India, another urban site in south Asia,
680 where the morning/evening values were lowest (0.9/19.5) in monsoon and highest in winter
681 (14.3/47.2) (Chandra et al., 2016). In the morning period, the ratio generally falls within a
682 narrower range, from less than 1 to about 25, which indicates a few dominant sources, such as
683 cooking, diesel vehicles, and diesel gen-sets (see Figure 9). In the evening period, the range of
684 the ratio is much wider, from less than 1 to more than 100, especially in winter. This is partly due
685 to the shallower boundary layer in winter, giving local CO emissions a chance to build up more

686 rapidly compared to the longer-lived and well-mixed CO₂, and also indicating the prevalence of
687 additional sources such as brick kilns and agro-residue burning.

688 **3.6 Comparison of CH₄ and CO₂ at semi-urban site (Bode) and rural site (Chanban)**

689 Figure 10 shows time series of hourly average mixing ratios of CH₄, CO₂, CO and water vapor
690 observed simultaneously at Bode and Chanban for the period of 15th July to 3rd October 2015.
691 The hourly meteorological parameters observed at Chanban are shown in supplementary Figure
692 S4. The hourly temperature ranges from 14 to 28.5 °C during the observation period. The site
693 experienced calm winds during the night and moderate southeasterly winds with hourly
694 maximum speed of up to 7.5 m s⁻¹ during the observation period. The CH₄ mixing ratios at
695 Chanban varied from 1.880 ppm to 2.384 ppm, and generally increased from the last week of
696 July until early September, peaking around 11th September and then falling off towards the end
697 of the month. CO followed a generally similar pattern, with daily average values ranging from
698 0.10 ppm to 0.28 ppm. The hourly CO₂ mixing ratios ranged from 375 to 453 ppm, with day to
699 day variations, but there were no clear pattern as observed in trend like CH₄ and CO mixing
700 ratios.

701 The CH₄, CO₂, and CO mixing ratios were higher in Bode than in Chanban (Figure 10, Table 4),
702 with Chanban approximately representing the baseline of the lower envelope of the Bode levels.
703 The mean CO₂, CH₄ and CO mixing ratios over the entire sampling period of nearly three
704 months at Bode are 3.8%, 12.1%, and 64% higher, respectively, than at Chanban. The difference
705 in the CO₂ mixing ratio could be due to the large uptake of CO₂ in the forested area at Chanban
706 and surrounding regions compared to Bode, where the local anthropogenic emissions rate is
707 higher and less vegetation for photosynthesis. The coincidence between the base values of CO
708 and CH₄ mixing ratios at Bode and the levels observed at Chanban implies that Chanban CO and
709 CH₄ mixing ratios are indicative of the regional background levels. A similar increase in CO and
710 CH₄ mixing ratios at Chanban from July to September was also observed at Bode, which may
711 imply that the regional/background levels in the broader Himalayan foothill region also
712 influences the baseline of the daily variability of the pollutants in the Kathmandu Valley,
713 consistent with Panday and Prinn (2009).

714 Figure 11 shows the comparison of average diurnal cycles of CO₂, CH₄, CO and water vapor
715 mixing ratios observed at Bode and Chanban. The diurnal pattern of CO₂ mixing ratios at both
716 sites is similar, but more pronounced at Bode, with a morning peak around 6:00-7:00, a daytime
717 minimum, and a gradual increase in the evening until the next morning peak. A prominent
718 morning peak at Bode during the monsoon season indicates the influence of local emission
719 sources. The daytime CO₂ mixing ratios are also higher at Bode than at Chanban because of local
720 emissions less uptake of CO₂ for photosynthesis in the valley in comparison to the forested area
721 around Chanban. Like the diurnal pattern of CO₂ depends on the evolution of the mixing layer at
722 Bode, as discussed earlier, it is expected that the mixing layer evolution similarly influences the
723 diurnal CO₂ mixing ratios at Chanban. CO, on the other hand, shows very different diurnal
724 patterns at Bode and Chanban. Sharp morning and evening peaks of CO are seen at Bode,
725 indicating the strong local polluting sources, especially cooking and traffic in the morning and
726 evening peak hours. Chanban, in contrast, only has a subtle morning peak and no evening peak.
727 After the morning peak, CO sharply decreases at Bode but not at Chanban. The growth of the
728 boundary layer after sunrise and entrainment of air from the free troposphere, with lower CO
729 mixing ratios, causes CO to decrease sharply during the day at Bode. At Chanban, on the other
730 hand, since the mixing ratios are already more representative of the local and regional
731 background levels which will also be prevalent in the lower free troposphere, CO does not
732 decrease notably during the daytime growth of the boundary layer as observed at Bode.

733 Similarly, while there is very little diurnal variation in the CH₄ mixing ratios at Chanban, there is
734 a strong diurnal cycle of CH₄ at Bode, similar to CO₂ there. At Chanban, the CH₄ mixing ratio
735 only shows a weak minimum at around 11 am, a slow increase during the day until a its peak
736 around 22:00, followed by a slow decrease during the night and a more rapid decrease through
737 the morning. The cause of this diurnal pattern at Chanban is presently unclear, but the levels
738 could be representative of the regional background throughout the day and show only limited
739 influences of local emissions.

740

741 4. Conclusions

742 A cavity ring down spectrometer (Picarro G2401, USA) was used to measure ambient CO₂, CH₄,
743 CO, and water vapor mixing ratios at a semi-urban site (Bode) in the Kathmandu Valley for a
744 year. This was the first 12-months of continuous measurements of these four species in the
745 Kathmandu Valley in the foothills of the central Himalaya. Simultaneous measurement was
746 carried out at a rural site (Chanban) for approximately 3 months to evaluate urban-rural
747 differences.

748 The measurement also provided an opportunity to establish diurnal and seasonal variation of
749 these species in one of the biggest metropolitan cities in the foothills of Himalayas. Annual
750 average of the mixing ratio of CH₄ and CO₂ in Bode revealed that they were higher than the
751 mixing ratios at the background sites such as the Mauna Loa, USA and Mt. Waliguan, China, as
752 well as higher than urban/semi-urban sites in nearby regions such as Ahmedabad and Shadnagar
753 in India. These comparisons highlight potential sources of CH₄ and CO₂ in the Kathmandu
754 Valley, such as brick kilns in the valley.

755 Polluted air masses were transported to the site mainly by two major local wind circulation
756 patterns, East-South/North East and West-Southwest throughout the observation period. Strong
757 seasonality was observed with CO compared to CO₂ and CH₄. Winter and pre-monsoon high CO
758 are linked to emission sources active in these seasons only and are from east-southeast and west-
759 southwest. Emission from the east-southeast are most likely related to brick kilns (winter and
760 pre-monsoon), which are in close proximity to Bode. Major city-centers are located in the west-
761 southwest of Bode (vehicular emission) which impact the site all-round the year, although higher
762 during winter season. Winter high was also observed with CO₂ and CH₄, which are mostly local
763 influence of brick kilns, trash burning and emission from city-center. Nighttime and early
764 morning accumulation of pollutants in winter due to a shallow stable mixing height (ca. 200 m)
765 also contribute to elevated levels than other seasons. Diurnal variation across all seasons
766 indicates the influence of rush-hour emissions related to vehicles and residential emissions. The
767 evolution of the mixing layer height (200-1200 m) was a major factor which controls the
768 morning-evening peak, afternoon low and night-early morning accumulation or decay. Thus the
769 geographical setting of the Kathmandu Valley and its associated meteorology play a key role in
770 the dispersion and ventilation of pollutants in the Kathmandu Valley. The ratio of CO/CO₂

771 across different season and wind direction showed that emissions from inefficient gasoline
772 vehicles, brick kilns, residential cooking and diesel combustion are likely to impact Bode.

773 The differences in mean values for urban-rural measurements at Bode and Chanban is highest for
774 CO (64 %) compared to CO₂ (3.8%) and CH₄ (12%). Low values of CH₄ and CO₂ mixing ratios
775 at the Chanban site could represent regional background mixing ratios.

776 This study has provided valuable information on key greenhouse gases and air pollutants in the
777 Kathmandu Valley and the surrounding regions. These observations can be useful as ground-
778 truthing for evaluation of satellite measurements, as well as climate and regional air quality
779 models. The overall analysis presented in the paper will contribute along with other recent
780 measurement and analysis to providing a sound scientific basis for reducing emissions of
781 greenhouse gases and air pollutants in the Kathmandu Valley.

782

783 **Acknowledgements**

784 The IASS is grateful for its funding from the German Federal Ministry for Education and
785 Research (BMBF) and the Brandenburg Ministry for Science, Research and Culture (MWFK).
786 This study was partially supported by core funds of ICIMOD contributed by the governments of
787 Afghanistan, Australia, Austria, Bangladesh, Bhutan, China, India, Myanmar, Nepal, Norway,
788 Pakistan, Switzerland, and the United Kingdom as well as funds provided to ICIMOD's
789 Atmosphere Initiative by the Governments of Sweden and Norway. We are thankful to
790 Bhogendra Kathayat, Shyam Newar, Dipesh Rupakheti, Piyush Bhardwaj, Ravi Pokharel, and
791 Pratik Singdan for their assistance during the measurement, P.S. Praveen for his support in
792 calibration of Picarro instrument, Pankaj Sadavarte for his help in refining Figure 1, and Liza
793 Manandhar and Rishi KC for the logistical support. The authors also express their appreciation to
794 the Department of Hydrology and Meteorology (DHM), Nepal, and the Nepal Army.

795

796 **References**

797

798 Aryal, R. K., Lee, B.-K., Karki, R., Gurung, A., Baral, B., and Byeon, S.-H.: Dynamics of PM
799 2.5 concentrations in Kathmandu Valley, Nepal, *J. Hazard. Mat.*, 168, 732-738, 2009.

800

801 Automotive Research Association of India (ARAI): Emission factor development for Indian
802 vehicles (http://www.cpcb.nic.in/Emission_Factors_Vehicles.pdf), 2008.

803

804 Brun, V. (Eds. 1): Fried earth bricks, kilns and workers in Kathmandu Valley. Himal Books,
805 Lazimpat-Kathmandu, Nepal, 2013.

806

807 Central Bureau of Statistics (CBS): Nepal Living Standards Survey 2010/11, Statistical Report
808 Volume 1, Central Bureau of Statistics, Government of Nepal, 2011.

809

810 Chandra, N., Lal, S., Venkataramani, S., Patra, P. K., and Sheel, V.: Temporal variations of
811 atmospheric CO₂ and CO at Ahmedabad in western India, *Atmos. Chem. Phys.*, 16, 6153-6173,
812 2016.

813

814 Chen, H., Karion, A., Rella, C., Winderlich, J., Gerbig, C., Filges, A., Newberger, T., Sweeney,
815 C., and Tans, P.: Accurate measurements of carbon monoxide in humid air using the cavity ring-
816 down spectroscopy (CRDS) technique, *Atmos. Meas. Tech.*, 6, 1031-1040, 2013.

817

818 Chen, P., Kang, S., Li, C., Rupakheti, M., Yan, F., Li, Q., Ji, Z., Zhang, Q., Luo, W., and
819 Sillanpää, M.: Characteristics and sources of polycyclic aromatic hydrocarbons in atmospheric
820 aerosols in the Kathmandu Valley, Nepal, *Sci. Total Environ.*, 538, 86-92, 2015.

821

822 Chen, Y. H., and Prinn, R. G.: Estimation of atmospheric methane emissions between 1996 and
823 2001 using a three-dimensional global chemical transport model, *J. Geophys. Res. Atmos.*, 111,
824 2006.

825
826 Conrad, R.: Soil microorganisms as controllers of atmospheric trace gases (H₂, CO, CH₄, OCS,
827 N₂O, and NO), *Microbiol. Rev.*, 60, 609-640, 1996.

828 Crosson, E.: A cavity ring-down analyzer for measuring atmospheric levels of methane, carbon
829 dioxide, and water vapor, *Appl. Phys. B: Lasers and Optics*, 92, 403-408, 2008.

830
831 Department of Transport Management (DoTM).: Annual report of Ministry of Labor and
832 transport management, Nepal Government, 2015.

833
834 Dlugokencky, E.J., A.M. Croswell, P.M. Lang, J.W. Mund, Atmospheric Methane Dry Air Mole
835 Fractions from quasi-continuous measurements at Mauna Loa, Hawaii, 1986-2016, Version:
836 2017-01-20, path: ftp://aftp.cmdl.noaa.gov/data/trace_gases/ch4/in-situ/surface/, 2017.

837
838 Dlugokencky, E.J., Lang, P.M., Croswell, A. M., Mund, J. W., Croswell, M. J., and Thoning, K.
839 W.: Atmospheric Methane Dry Air Mole Fractions from the NOAA ESRL Carbon Cycle
840 Cooperative Global Air Sampling Network, 1983-2015, Version: 2016-07-07, Path:
841 ftp://aftp.cmdl.noaa.gov/data/trace_gases/ch4/flask/surface/, 2016.

842
843 Dlugokencky, E.J., Lang, P.M., Mund, J.W., Croswell, A. M., Croswell, M. J., and Thoning, K.
844 W.: Atmospheric Carbon Dioxide Dry Air Mole Fractions from the NOAA ESRL Carbon Cycle
845 Cooperative Global Air Sampling Network, 1968-2015, Version: 2016-08-30, Path:
846 ftp://aftp.cmdl.noaa.gov/data/trace_gases/co2/flask/surface/, 2016a.

847
848 Fowler, A., and Hennessy, K.: Potential impacts of global warming on the frequency and
849 magnitude of heavy precipitation, *Nat. Hazards*, 11, 283-303, 1995.

850
851 Fragkias, M., Lobo, J., Strumsky, D., and Seto, K. C.: Does size matter? Scaling of CO₂
852 emissions and US urban areas, *PLoS One*, 8, e64727, 2013.

853

854 Ganesan, A., Chatterjee, A., Prinn, R., Harth, C., Salameh, P., Manning, A., Hall, B., Mühle, J.,
855 Meredith, L., and Weiss, R.: The variability of methane, nitrous oxide and sulfur hexafluoride in
856 Northeast India, *Atmos. Chem. Phys.*, 13, 10633-10644, 2013.

857

858 Goroshi, S. K., Singh, R., Panigrahy, S., and Parihar, J.: Analysis of seasonal variability of
859 vegetation and methane concentration over India using SPOT-VEGETATION and ENVISAT-
860 SCIAMACHY data, *J. Indian Soc. Remote*, 39, 315-321, 2011.

861

862 International Centre for Integrated Mountain Development (ICIMOD): Himalayas – Water for
863 1.3 Billion People. ICIMOD, Lalitpur, 2009.

864 Intergovernmental Panel for Climate Change (IPCC): Climate Change 2013: The Physical
865 Science Basis. Contribution of Working Group I to the Fifth Assessment Report of the
866 Intergovernmental Panel on Climate Change, Cambridge University Press, Cambridge, United
867 Kingdom and New York, NY, USA, 2013.

868

869 Kim, B. M., Park, J.-S., Kim, S.-W., Kim, H., Jeon, H., Cho, C., Kim, J.-H., Hong, S.,
870 Rupakheti, M., and Panday, A. K.: Source apportionment of PM 10 mass and particulate carbon
871 in the Kathmandu Valley, Nepal, *Atmos. Environ.*, 123, 190-199, 2015.

872

873 Kitada, T., and Regmi, R. P.: Dynamics of air pollution transport in late wintertime over
874 Kathmandu Valley, Nepal: As revealed with numerical simulation, *J. Appl. Meteorol.*, 42, 1770-
875 1798, 2003.

876

877 Kumar, M. K., and Nagendra, S. S.: Characteristics of ground level CO₂ concentrations over
878 contrasting land uses in a tropical urban environment, *Atmos. Environ.*, 115, 286-294, 2015.

879

880 Marinoni, A., Cristofanelli, P., Laj, P., Duchi, R., Putero, D., Calzolari, F., Landi, T.,
881 Vuillermoz, E., Maione, M., and Bonasoni, P.: High black carbon and ozone concentrations

882 during pollution transport in the Himalayas: Five years of continuous observations at NCO-P
883 global GAW station, *J. Environ. Sci.*, 25, 1618-1625, 2013.

884

885 Ministry of Environment (MoE).: Status of climate change in Nepal, Kathmandu Nepal.
886 Kathmandu, Ministry of Environment, 2011.

887 Ministry of Environment and Forest (MoEF).: Indian Network for Climate Change Assessment:
888 India: Greenhouse Gas Emissions 2007, Tech. rep., 2007.

889 Mues, A., Rupakheti, M., Münkkel, C., Lauer, A., Bozem, H., Hoor, P., Butler, T., and Lawrence,
890 M.: Investigation of the mixing layer height derived from ceilometer measurements in the
891 Kathmandu Valley and implications for local air quality. *Atmos. Chem. Phys.*, doi:10.5194/acp-
892 2016-1002, in press, 2017.

893

894 Nepal Electricity Authority (NEA).: A year in review - fiscal year - 2013/2014
895 (http://www.nea.org.np/images/supportive_docs/Annual%20Report-2014.pdf), 2014.

896 NOAA ESRL Global Monitoring Division. updated annually.: Atmospheric Carbon Dioxide Dry
897 Air Mole Fractions from quasi-continuous measurements at Mauna Loa, Hawaii. Compiled by
898 K.W. Thoning, D.R. Kitzis, and A. Crotwell. National Oceanic and Atmospheric Administration
899 (NOAA), Earth System Research Laboratory (ESRL), Global Monitoring Division (GMD):
900 Boulder, Colorado, USA. Version 2016-8 at <http://dx.doi.org/10.7289/V54X55RG>, 2015.

901

902 Panday, A. K., and Prinn, R. G.: Diurnal cycle of air pollution in the Kathmandu Valley, Nepal:
903 Observations, *J. Geophys. Res.: Atmos.*, 114, 2009.

904

905 Panday, A. K., Prinn, R. G., and Schär, C.: Diurnal cycle of air pollution in the Kathmandu
906 Valley, Nepal: 2. Modeling results, *Journal of Geophysical Research: Atmospheres*, 114, 2009.

907 Patra, P., Niwa, Y., Schuck, T., Brenninkmeijer, C., Machida, T., Matsueda, H., and Sawa, Y.:
908 Carbon balance of South Asia constrained by passenger aircraft CO₂ measurements, *Atmos.*
909 *Chem. Phys.*, 11, 4163-4175, 2011.

910
911 Pandey, A., Sadavarte, P., Rao, A. B., Venkataraman C.: Trends in multipollutant emissions
912 from a technology-linked inventory for India: II. Residential, agricultural and informal industry
913 sectors, *Atmos. Environ.*, 99, 341-352, doi: 10.1016/j.atmosenv.2014.09.080, 2014.

914 Patra, P., Canadell, J., Houghton, R., Piao, S., Oh, N.-H., Ciais, P., Manjunath, K., Chhabra, A.,
915 Wang, T., and Bhattacharya, T.: The carbon budget of South Asia, 2013.

916
917 Patra, P., Niwa, Y., Schuck, T., Brenninkmeijer, C., Machida, T., Matsueda, H., and Sawa, Y.:
918 Carbon balance of South Asia constrained by passenger aircraft CO₂ measurements, *Atmos.*
919 *Chem. Phys.*, 11, 4163-4175, 2011.

920
921 Picarro.: Picarro G2401 CO₂, CH₄, CO, Water vapor CRDS analyzer
922 ([http://hpst.cz/sites/default/files/attachments/datasheet-g2401-crds-analyzer-co2-co-ch4-h2o-air-](http://hpst.cz/sites/default/files/attachments/datasheet-g2401-crds-analyzer-co2-co-ch4-h2o-air-oct15-1.pdf)
923 [oct15-1.pdf](http://hpst.cz/sites/default/files/attachments/datasheet-g2401-crds-analyzer-co2-co-ch4-h2o-air-oct15-1.pdf)), 2015.

924
925 Prasad, P., Rastogi, S., and Singh, R.: Study of satellite retrieved CO₂ and CH₄ concentration
926 over India, *Adv. Space Res.*, 54, 1933-1940, 2014.

927
928 Pudasainee, D., Sapkota, B., Shrestha, M. L., Kaga, A., Kondo, A., and Inoue, Y.: Ground level
929 ozone concentrations and its association with NO_x and meteorological parameters in Kathmandu
930 valley, Nepal, *Atmos. Environ.*, 40, 8081-8087, 2006.

931
932 Putero, D., Landi, T., Cristofanelli, P., Marinoni, A., Laj, P., Duchi, R., Calzolari, F., Verza, G.,
933 and Bonasoni, P.: Influence of open vegetation fires on black carbon and ozone variability in the
934 southern Himalayas (NCO-P, 5079 m asl), *Environ. Pollut.*, 184, 597-604, 2014.

935
936 Putero, D., Cristofanelli, P., Marinoni, A., Adhikary, B., Duchi, R., Shrestha, S., Verza, G.,
937 Landi, T., Calzolari, F., and Busetto, M.: Seasonal variation of ozone and black carbon observed

938 at Paknajol, an urban site in the Kathmandu Valley, Nepal, *Atmos. Chem. Phys.*, 15, 13957-
939 13971, 2015.

940

941 Regmi, R. P., Kitada, T., and Kurata, G.: Numerical simulation of late wintertime local flows in
942 Kathmandu valley, Nepal: Implication for air pollution transport, *J. Appl. Meteorol.*, 42, 389-
943 403, 2003.

944

945 Rodda, S.R., Thumaty, K. C., Jha, C. S. and Dadhwal, V. K.: Seasonal Variations of Carbon
946 Dioxide, Water Vapor and Energy Fluxes in Tropical Indian Mangroves. *Forests*, 7, 35;
947 doi:10.3390/f7020035, 2016.

948

949 Rupakheti, M., Panday, A. K., Lawrence, M. G., Kim, S. W., Sinha, V., Kang, S. C., Naja, M.,
950 Park, J. S., Hoor, P., Holben, B., Sharma, R. K., Mues, A., Mahata, K. S., Bhardwaj, P., Sarkar,
951 C., Rupakheti, D., Regmi, R. P., and Gustafsson, Ö.: Air pollution in the Himalayan foothills:
952 overview of the SusKat-ABC international air pollution measurement campaign in Nepal,
953 *Atmos. Chem. Phys.*, in preparation, 2017.

954

955 Sahu, L. K., and Lal, S.: Distributions of C₂–C₅ NMHCs and related trace gases at a tropical
956 urban site in India. *Atmos. Environ.*, 40(5), 880-891, 2006.

957

958 Sarangi, T., Naja, M., S.Lal, Venkataramani, S., Bhardwaj, P., Ojha, N., Kumar, R., Chandola,
959 H. C.: First observations of light non-methane hydrocarbons (C₂–C₅) over a high altitude site in
960 the central Himalayas, *Atmos. Environ.*, 125, 450–460, 2016.

961

962 Sarangi T., Naja, M., Ojha, N., Kumar, R., Lal, S., Venkataramani, S., Kumar, A., Sagar, R., and
963 Chandola, H. C.: First simultaneous measurements of ozone, CO and NO_y at a high altitude
964 regional representative site in the central Himalayas, *J. Geophys. Res.*, 119,
965 doi:10.1002/2013JD020631, 2014.

966

967 Sarkar, C., Sinha, V., Kumar, V., Rupakheti, M., Panday, A., Mahata, K. S., Rupakheti, D.,
968 Kathayat, B., and Lawrence, M. G.: Overview of VOC emissions and chemistry from PTR-TOF-
969 MS measurements during the SusKat-ABC campaign: high acetaldehyde, isoprene and isocyanic
970 acid in wintertime air of the Kathmandu Valley, *Atmos. Chem. Phys.*, 16, 3979-4003, 2016.
971

972 Schneising, O., Buchwitz, M., Burrows, J., Bovensmann, H., Bergamaschi, P., and Peters, W.:
973 Three years of greenhouse gas column-averaged dry air mole fractions retrieved from satellite-
974 Part 2: Methane, *Atmos. Chem. Phys.*, 9, 443-465, 2009.
975

976 Sharma, R., Bhattarai, B., Sapkota, B., Gewali, M., and Kjeldstad, B.: Black carbon aerosols
977 variation in Kathmandu valley, Nepal, *Atmos. Environ.*, 63, 282-288, 2012.
978

979 Shrestha, R. M., and Rajbhandari, S.: Energy and environmental implications of carbon emission
980 reduction targets: Case of Kathmandu Valley, Nepal, *Energ. Policy*, 38, 4818-4827, 2010.
981

982 Shrestha, S. R., Oanh, N. T. K., Xu, Q., Rupakheti, M., and Lawrence, M. G.: Analysis of the
983 vehicle fleet in the Kathmandu Valley for estimation of environment and climate co-benefits of
984 technology intrusions, *Atmos. Environ.*, 81, 579-590, 2013.
985

986 Sinha, V., Kumar, V., and Sarkar, C.: Chemical composition of pre-monsoon air in the Indo-
987 Gangetic Plain measured using a new air quality facility and PTR-MS: high surface ozone and
988 strong influence of biomass burning, *Atmos. Chem. Phys.*, 14, 5921-5941, 10.5194/acp-14-5921-
989 2014, 2014.
990

991 Smith, K. R., Uma, R., Kishore, V., Zhang, J., Joshi, V., and Khalil, M.: Greenhouse
992 implications of household stoves: an analysis for India, *Ann. Rev. Energy and the Environ.*, 25,
993 741-763, 2000.
994

995 Sreenivas, G., Mahesh, P., Subin, J., Kanchana, A. L., Rao, P. V. N., and Dadhwal, V. K.:
996 Influence of Meteorology and interrelationship with greenhouse gases (CO₂ and CH₄) at a
997 suburban site of India, *Atmos. Chem. Phys.*, 16, 3953-3967, 2016.
998

999 Stockwell, C. E., Christian, T. J., Goetz, J. D., Jayarathne, T., Bhave, P. V., Praveen, P. S.,
1000 Adhikari, S., Maharjan, R., DeCarlo, P. F., and Stone, E. A.: Nepal ambient monitoring and
1001 source testing experiment (NAMaSTE): emissions of trace gases and light-absorbing carbon
1002 from wood and dung cooking fires, garbage and crop residue burning, brick kilns, and other
1003 sources, *Atmos. Chem. Phys.*, 16, 11043-11081, 2016.
1004

1005 Westerdahl, D., Wang, X., Pan, X., and Zhang, K. M.: Characterization of on-road vehicle
1006 emission factors and microenvironmental air quality in Beijing, China, *Atmos. Environ.*, 43, 697-
1007 705, 2009.
1008

1009 Weyant, C., Athalye, V., Ragavan, S., Rajarathnam, U., Lalchandani, D., Maithel, S., Baum, E.,
1010 and Bond, T. C.: Emissions from South Asian brick production, *Environ. Sci. Tech.*, 48, 6477-
1011 6483, 2014.
1012

1013 World Bank.: Managing Nepal's Urban Transition
1014 (<http://www.worldbank.org/en/news/feature/2013/04/01/managing-nepals-urban-transition>),
1015 2013.
1016

1017 World Bank.: Diesel power generation: inventories, black carbon emissions in Kathmandu
1018 Valley, Nepal. Washington. The World Bank: 1818H Street NW, Washington, DC 20433, USA

1019 WMO.: The state of greenhouse gases in the atmosphere based on global observations through
1020 2015(http://reliefweb.int/sites/reliefweb.int/files/resources/GHG_Bulletin_12_EN_web_JN1616
1021 40.pdf), 2016.
1022

Table 1. Instruments and sampling at Bode (semi-urban site) and Chanban (rural site)

Site	Instrument	Species	sampling interval	Measurement period	inlet/sensor height above ground (m)
Bode	i. Cavity ring down spectrometer (Picarro G2401, USA)	CO ₂ , CH ₄ , CO, water vapor	5 sec	06 Mar 2013 - 05 Mar 2014 14 Jul 2015 - 07 Aug 2015	20
	ii. CO monitor (Horriba AP370, USA)	CO	5 min	06 Mar 2013 – 07 June 2013	20
	iii. Ceilometer (Vaisala CL31, Finland)		15-52 min	06 Mar 2013 – 05 Mar 2014	15
	iv. AWS (Campbell Scientific, USA)		1 min		23
	a. CS215	RH, T		06 Mar 2013 – 24 Apr 2013	
	b. CS300 Pyranometer	SR		06 Mar 2013 - 05 Mar 2014 14 Jul 2015 - 07 Aug 2015	
	c. RM Young 05103-5	WD, WS		06 Mar 2013 - 05 Mar 2014 14 July 2015 - 07 Aug 2015	
	v. Airport AWS (Envirodata, Australia)				
	a. TA10	T		18 Jun 2013 – 13 Jan 2013	
	b. RG series	RF		06 Mar 2013 – 15 Dec 2013	
Chanban	i. Cavity ring down spectrometer (Picarro G2401, USA)	CO ₂ , CH ₄ , CO, water vapor	5 sec	15 July 2015 - 03 Oct 2015	3
	ii AWS (Davis Vantage Pro2, USA)	RH, T, SR, WD, WS, RF, P	10 min	14 July 2015 - 07 Aug 2015	2

AWS: Automatic weather station, RH: ambient relative humidity, T: ambient temperature, SR: global solar radiation, WS: wind speed, WD: wind direction, RF: rainfall, P: ambient pressure

Table 2. Summary of monthly average CH₄ and CO₂ mixing ratios observed at Bode, a semi-urban site in the Kathmandu Valley during March 2013 to Feb 2014 [mean, standard deviation (SD), median, minimum (Min.), maximum (Max.) and number of data points of hourly average values]

Month	CH ₄ (ppm)					CO ₂ (ppm)					Data points
	Mean	SD	Median	Min.	Max.	Mean	SD	Median	Min.	Max.	
Mar	2.207	0.245	2.152	1.851	3.094	426.6	26.4	418.3	378.8	510.8	596
Apr	2.183	0.252	2.094	1.848	3.121	430.3	27.4	421.0	397.0	536.9	713
May	2.093	0.174	2.040	1.863	2.788	421.7	22.1	413.4	395.9	511.2	725
Jun	2.061	0.142	2.017	1.869	2.675	417.9	21.3	410.4	390.5	495.7	711
Jul	2.129	0.168	2.074	1.893	2.770	410.3	18.2	406.3	381.0	471.0	500
Aug	2.274	0.260	2.181	1.953	3.219	409.9	22.8	405.3	376.1	493.1	737
Sep	2.301	0.261	2.242	1.941	3.331	414.9	30.2	404.0	375.9	506.2	710
Oct	2.210	0.195	2.156	1.927	2.762	417.0	25.1	411.8	381.9	486.7	743
Nov	2.207	0.203	2.178	1.879	2.705	417.2	20.7	415.7	385.7	478.9	717
Dec	2.206	0.184	2.193	1.891	2.788	417.7	17.3	418.0	386.7	467.6	744
Jan	2.233	0.219	2.198	1.889	2.744	424.8	20.9	422.3	392.7	494.5	696
Feb	2.199	0.223	2.152	1.877	2.895	423.2	22.0	417.9	392.2	484.6	658
Annual	2.192	0.066	2.140	1.848	3.331	419.3	6.0	413.7	375.9	536.9	

Table 3. Summary of CH₄ and CO₂ mixing ratios at Bode across four seasons during March 2013 to Feb 2014 [seasonal mean, one standard deviation (SD), median, minimum (Min.) and maximum (Max.)]

Season	CH ₄ (ppm)					CO ₂ (ppm)				
	Mean	SD	Median	Min.	Max.	Mean	SD	Median	Min.	Max.
Pre-Monsoon	2.157	0.230	2.082	1.848	3.121	426.2	25.5	417.0	378.8	536.9
Monsoon	2.199	0.241	2.126	1.869	3.331	413.5	24.2	407.1	375.9	506.2
Post-Monsoon	2.210	0.200	2.167	1.879	2.762	417.3	23.1	414.1	381.9	486.7
Winter	2.214	0.209	2.177	1.877	2.895	421.9	20.3	419.3	386.7	494.5

Table 4. Comparison of monthly average CH₄ and CO₂ mixing ratios at a semi-urban and a rural site in Nepal (this study) with other urban and background sites in the region and elsewhere.

Site Setting	Bode, Nepal (Urban)				Chanban, Nepal (Rural)		Mauna Loa, USA (Background) ^c		Waliguan, China (Background) ^d	
	CO ₂	CH ₄	*CO ₂	*CH ₄	*CO ₂	*CH ₄	CO ₂	CH ₄	CO ₂	CH ₄
Unit	ppm	ppm	ppm	ppm	ppm	ppm	ppm	ppm	ppm	ppm
Mar 2013	426.6	2.207					397.3	1.840	399.5	1.868
Apr	430.3	2.183					398.4	1.837	402.8	1.874
May	421.7	2.093					399.8	1.834	402.5	1.878
Jun	417.9	2.061					398.6	1.818	397.4	1.887
Jul	410.3	2.129					397.2	1.808	393.3	1.888
Aug	409.9	2.274	411.3	2.281	403.4	2.050	395.2	1.819	392.0	1.893
Sep	414.9	2.301	419.9	2.371	399.1	2.102	393.5	1.836	393.1	1.894
Oct	417.0	2.210					393.7	1.836	395.6	1.876
Nov	417.2	2.207					395.1	1.835	397.1	1.875
Dec	417.7	2.206					396.8	1.845	398.6	1.880
Jan 2014	424.8	2.234					397.8	1.842	398.8	1.865
Feb	423.2	2.199					397.9	1.834	401.1	1.878
<i>Annual</i>										
Bode	419.3	2.192								
Mauna Loa							396.8	1.832		
Waliguan									397.7	1.880
Shadnagar (2014) ^a	394.0									
Ahemadabad (2013-2015) ^b	413.0	1.920								

*The monthly values for CO₂ and CH₄ in 2015, ^aSreenivas et al., 2016, ^bChandra et al., 2016, ^cDlugokencky et al., 2017; NOAA, 2015, ^dDlugokencky et al., 2016; Dlugokencky et al., 2016a.

Table 5. Emission ratio of CO/CO₂ (ppb ppm⁻¹) derived from emission factors (gram of gas emitted from per kilogram of fuel burned, except transport sector which is derived from gram of gases emitted per kilometer distance travelled)

Sectors	Details	CO/CO ₂	Reference
1. Residential/Commercial			
i. LPG		4.8	Smith et al. (2000)
ii. Kerosene		13.4	Smith et al. (2000)
iii. Biomass		52.9 - 98.5	*
iv. Diesel power generators	< 15 year old	5.8	The World Bank (2014)
	>15 year old	4.5	
2. Transport			
a. Diesel			
i. HCV diesel bus	>6000cc, 1996-2000	4.9	
	post 2000 and 2005	5.4	
ii. HCV diesel truck	>6000cc, post 2000	7.9	
b. Petrol			
i. 4 stroke motorcycle	<100 cc, 1996-2000	68	
	100-200 cc, Post 2000	59.6	
ii. Passenger cars	<1000 cc, 1996-2000	42.4	
iii. Passenger cars	<1000 cc, Post 2000	10.3	
3. Brick industries			
i. BTK fixed kiln		17.2	Weyant et al. (2014)
ii. Clamp brick kiln		33.7	Stockwell et al. (2016)
iii. Zigzag brick kiln		3.9	Stockwell et al. (2016)
4. Open burning			
i. Mixed garbage		46.9	Stockwell et al. (2016)
ii. Crop-residue		51.6	Stockwell et al. (2016)

* Westerdahl et al. (2009)

** http://www.cpcb.nic.in/Emission_Factors_Vehicles.pdf

Table 6. Average (SD) of the ratio of dCO to dCO₂, their Geometric mean (GeoSD) over a period of 3 hours during (a) morning peak (b) evening peak and (c) seasonal (all hours) of the ambient mixing ratios of CO and CO₂. And their lower and upper bound (LB and UB).

Period	Season	Mean (SD)	Median	N	Geomean (GeoSD)	LB	UB
a. Morning hours (7:00-9:00)	Pre-monsoon	7.6 (3.1)	7.8	249	11.3 (1.5)	5.2	24.8
	Monsoon	2.2 (1.6)	1.9	324	9.9 (1.9)	2.7	36.3
	Post-monsoon	3.1 (1.4)	2.8	183	11.1 (1.5)	4.7	26.3
	Winter*	11.2 (4.4)	11	255	11.4 (1.5)	5.3	24.2
b. Evening hours (19:00-21:00)	Pre-monsoon	15.1 (9.0)	12.7	248	10.5 (1.7)	3.5	31.6
	Monsoon	8.0 (5.2)	6.3	323	10.2 (1.8)	3.1	33.5
	Post-monsoon	11.5 (5.6)	10.6	182	11.0 (1.6)	4.4	27.6
	Winter	21.6 (14.1)	18.2	254	10.2 (1.8)	3.1	33.6
c. Seasonal (all hours)	Pre-monsoon	12.2 (13.3)	8.8	1740	8.2 (2.4)	1.4	48.4
	Monsoon	7.5 (13.5)	2.9	2176	5.9 (3.3)	0.5	65.6
	Post-monsoon	8.3 (12.4)	4.4	1289	6.8 (3.0)	0.8	59.2
	Winter	15.1 (13.3)	12.5	1932	9.2 (2.1)	2.0	41.7

*The morning peak was one hour delayed in winter, thus the 8:00-10:00 period data was used in the analysis.

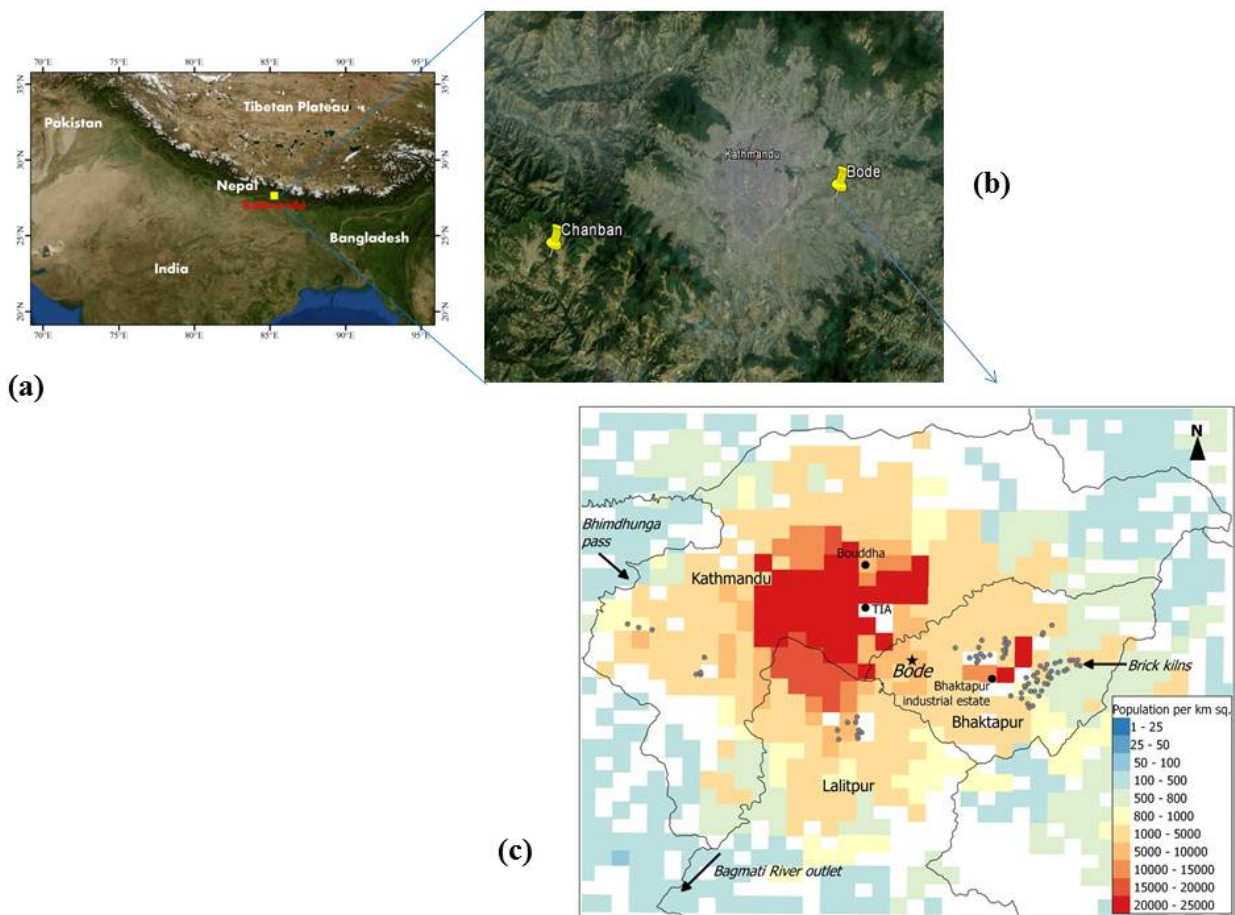


Figure 1. Location of measurement sites: (a) Kathmandu Valley (b) semi-urban measurement site at Bode in Kathmandu Valley, and a rural measurement site at Chanban in Makawanpur district Nepal, (c) general setting of Bode site. Colored grid and TIA represent population density and the Tribhuvan International Airport, respectively.

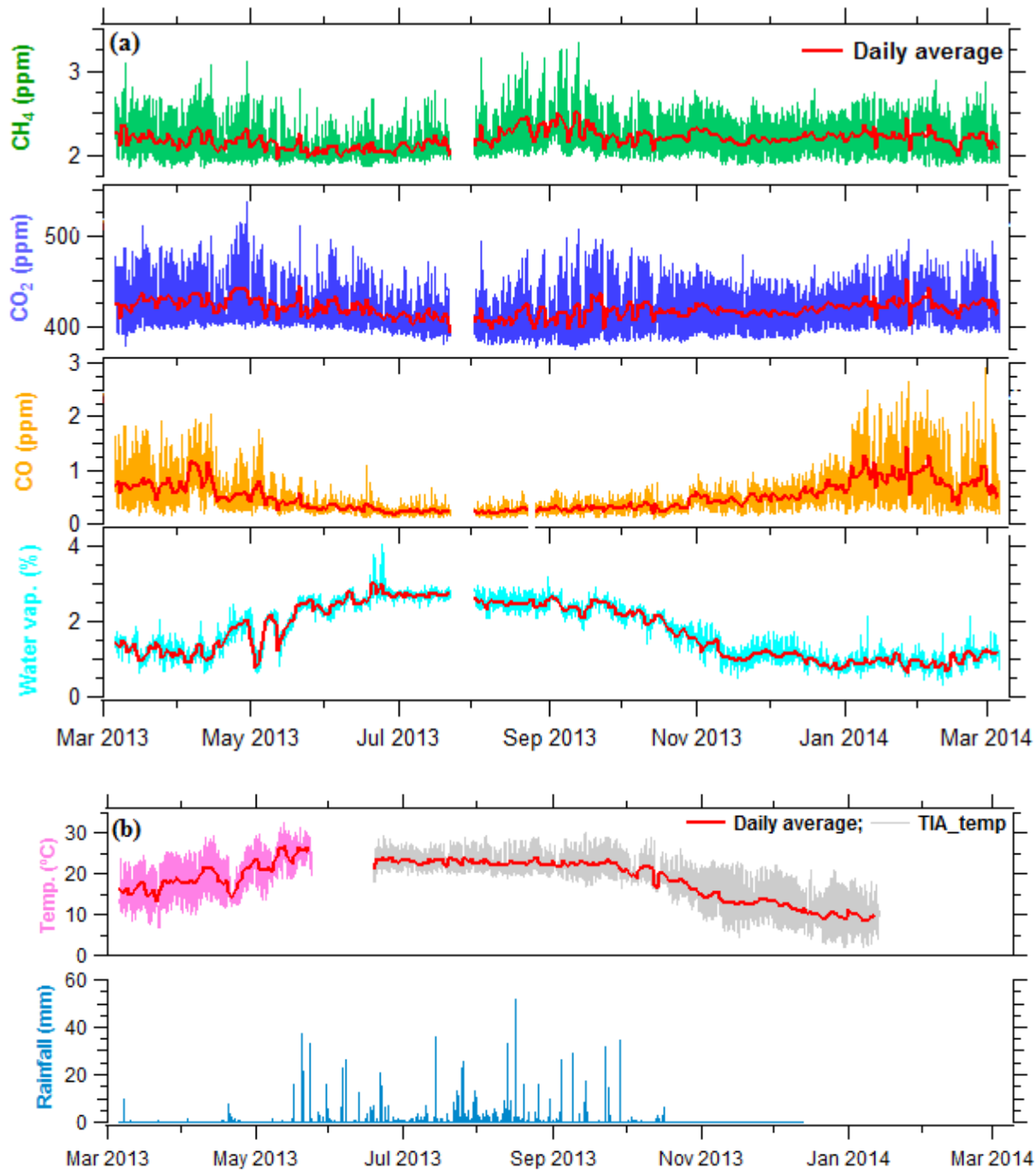


Figure 2. Time series of hourly average (a) mixing ratios of CH₄, CO₂, CO, and water vapor measured with a cavity ring down spectrometer (Picarro G2401) at Bode, and (b) temperature and rainfall monitored at the Tribhuvan International Airport (TIA), ~4 km to the west of Bode site in the Kathmandu Valley, Nepal. Temperature shown in pink color is observed at Bode site.

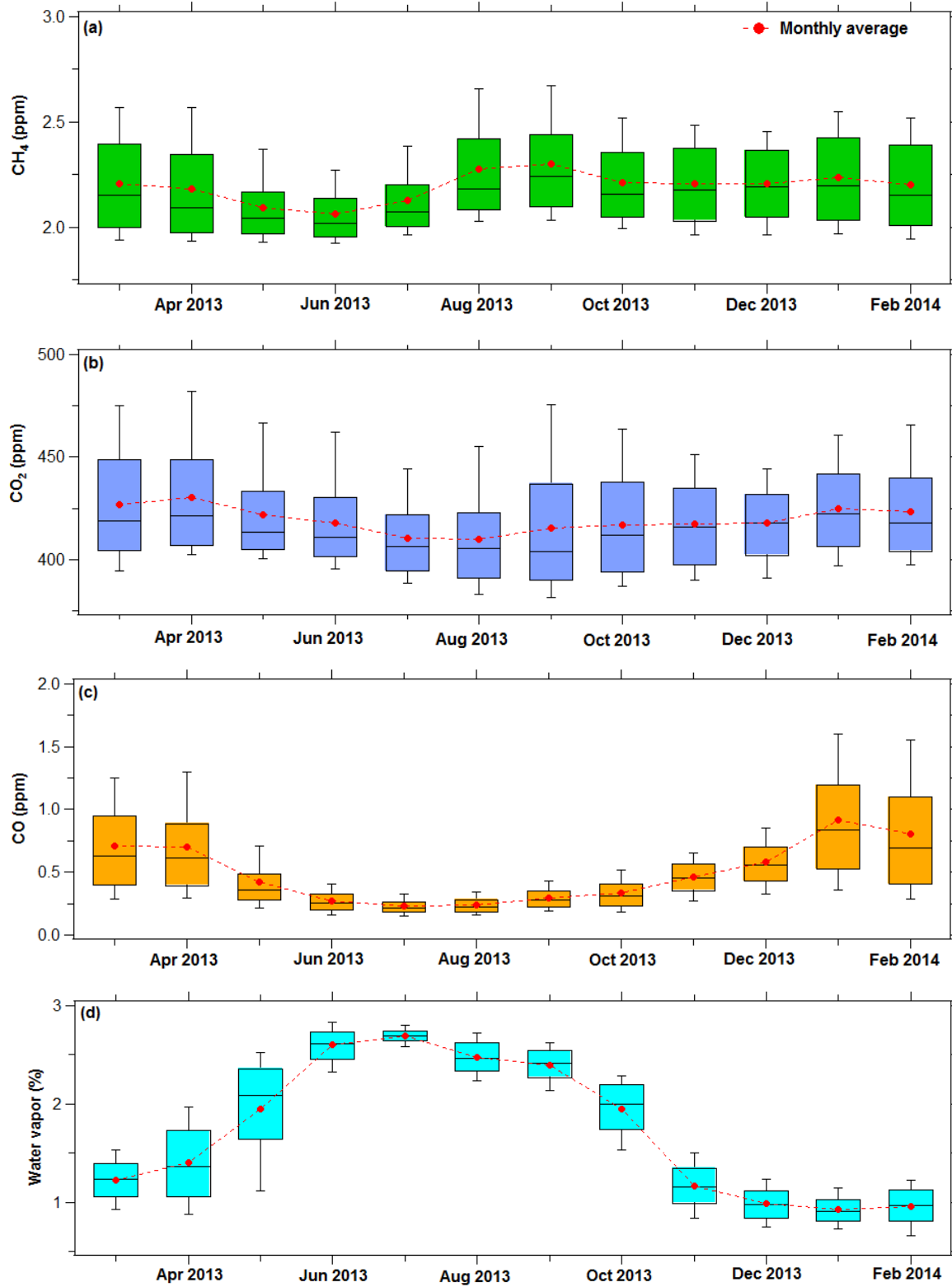
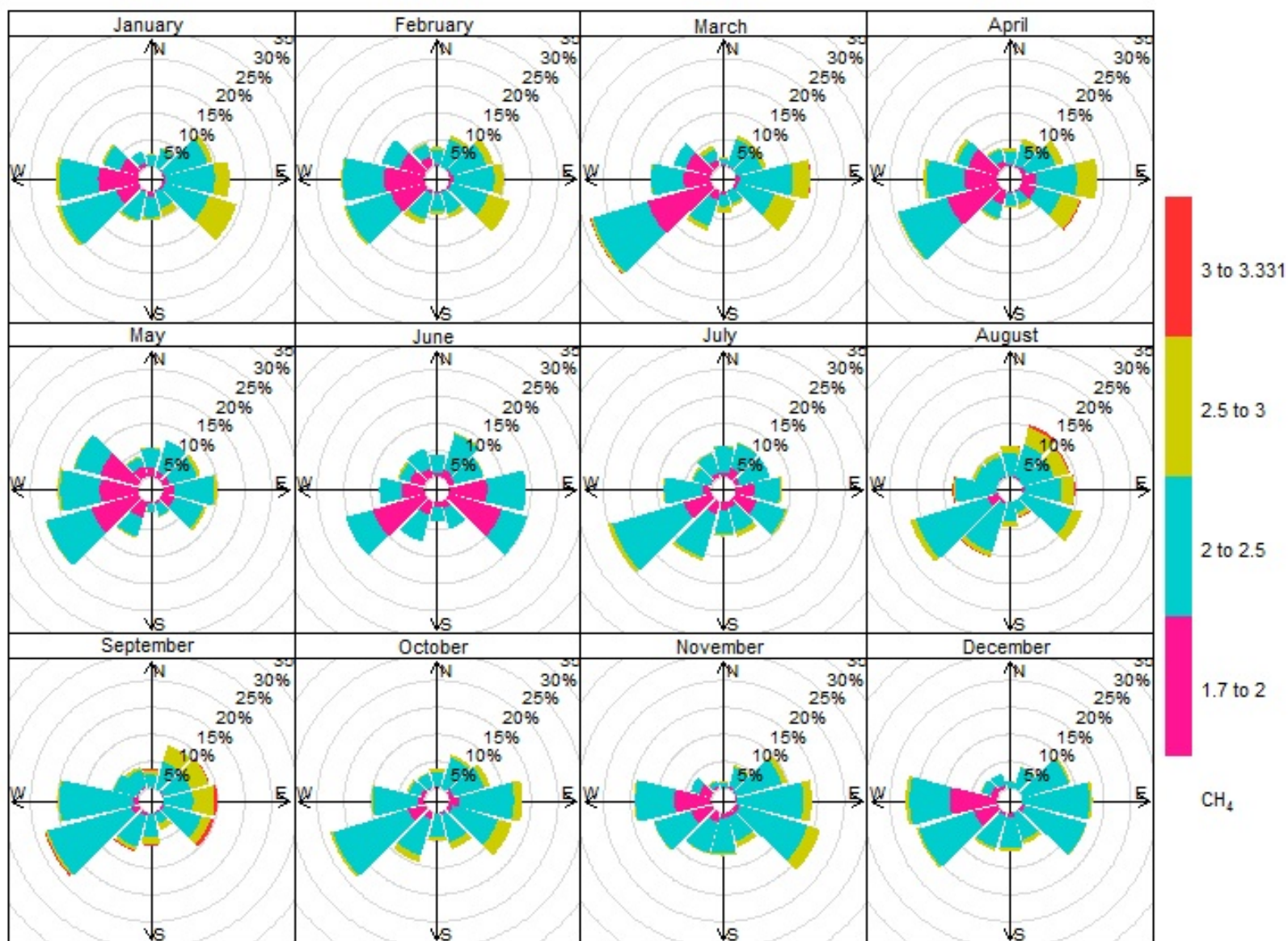
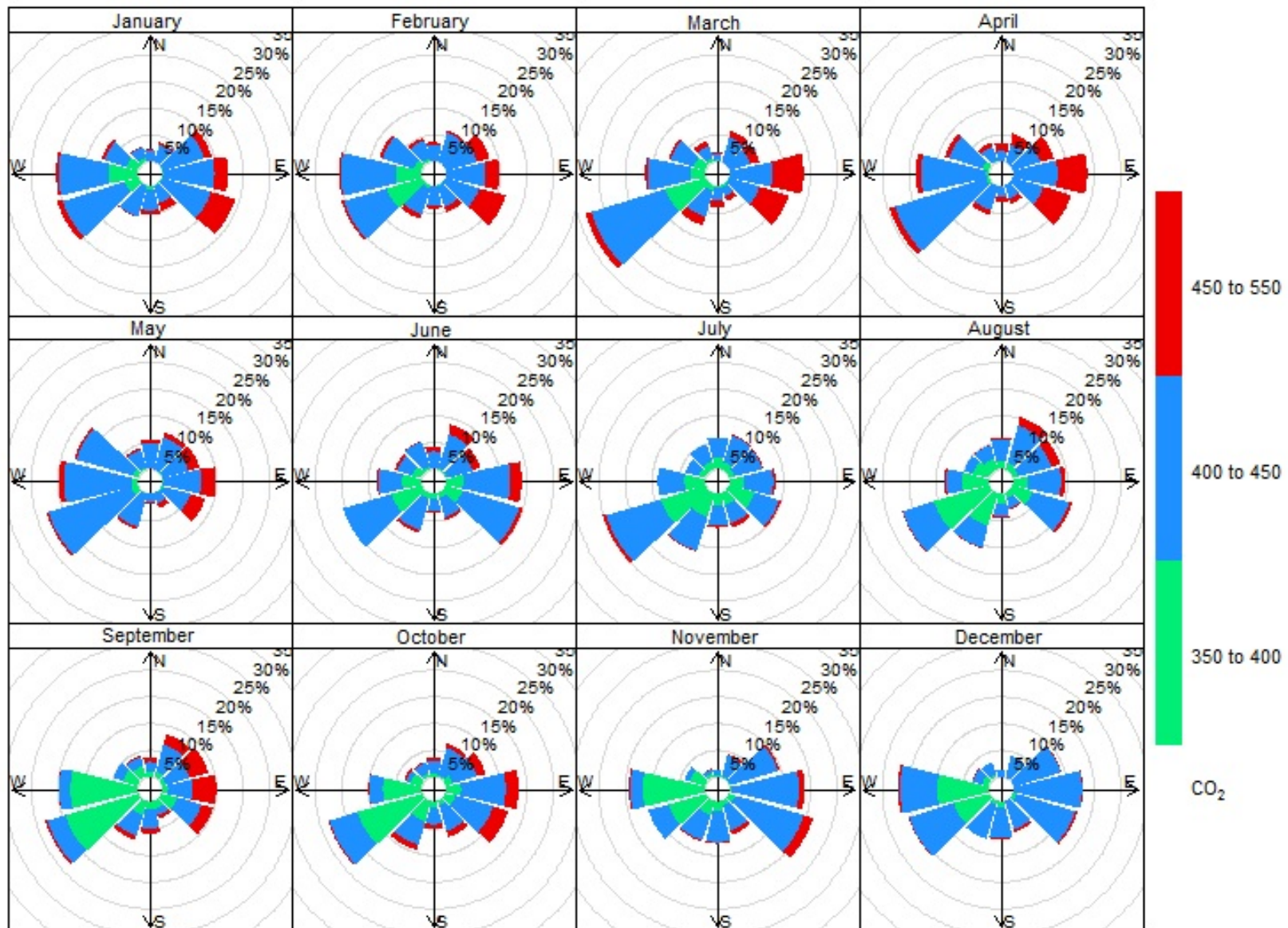


Figure 3. Monthly variations of the mixing ratios of hourly (a) CH₄, (b) CO₂, (c) CO, and (d) water vapor observed at a semi-urban site (Bode) in the Kathmandu Valley over a period of a year. The lower end and upper end of the whisker represents 10th and 90th percentile, respectively; the lower end and upper end of each box represents 25th and 75th percentile, respectively, and black horizontal line in the middle of each box is the median for each month while red dot represents mean for each month.

(a)



(b)



(c)

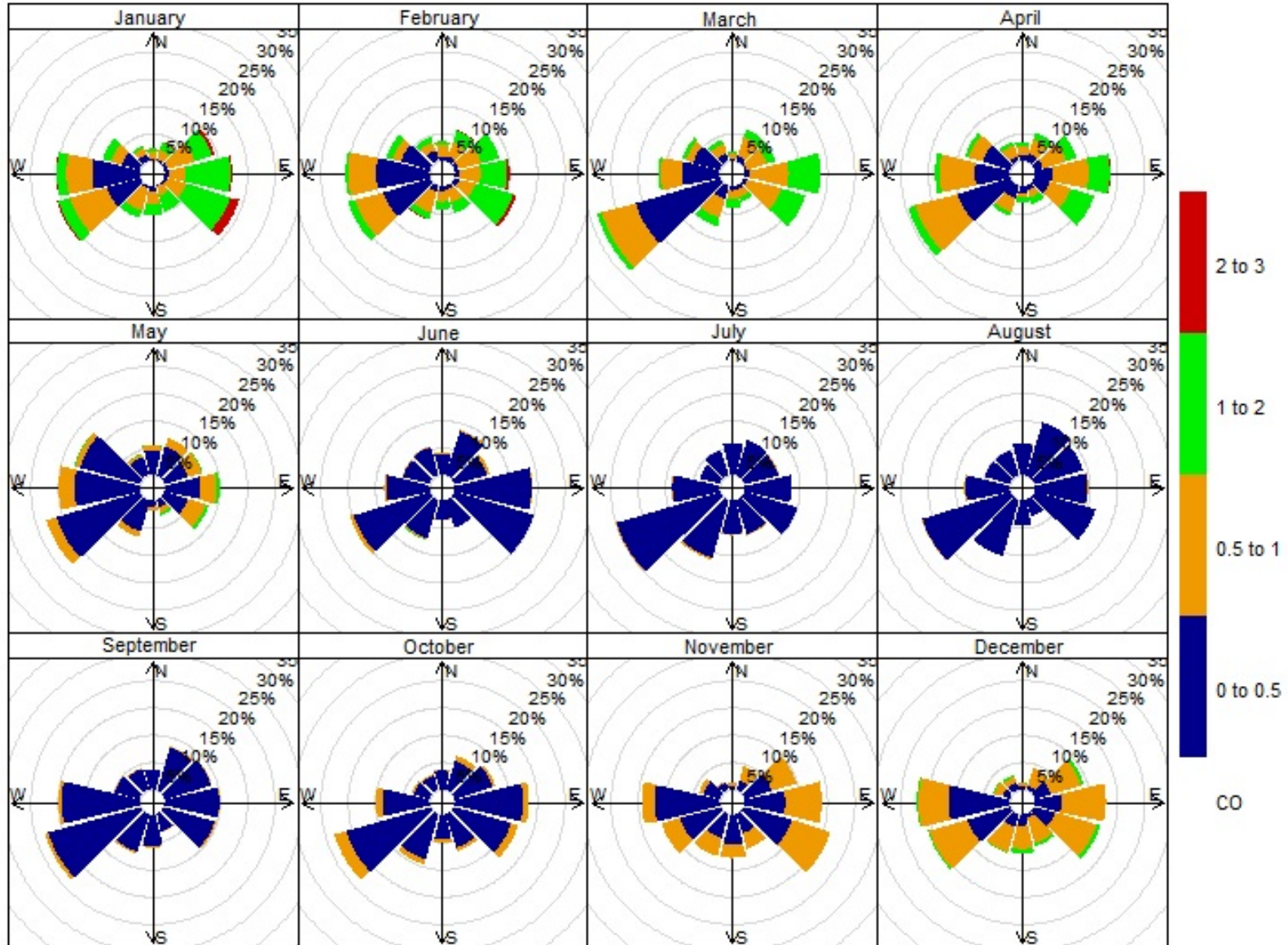


Figure 4. Relation between mixing ratios and wind direction observed at Bode in the Kathmandu Valley (a) CH₄, (b) CO₂ and (c) CO from March 2013 to February 2014. The figure shows variations of CH₄, CO₂ and CO mixing ratios based on frequency counts of wind direction (in %) as represented by circle. The color represents the different mixing ratios of the gaseous species. The units of CH₄, CO₂ and CO are in ppm.

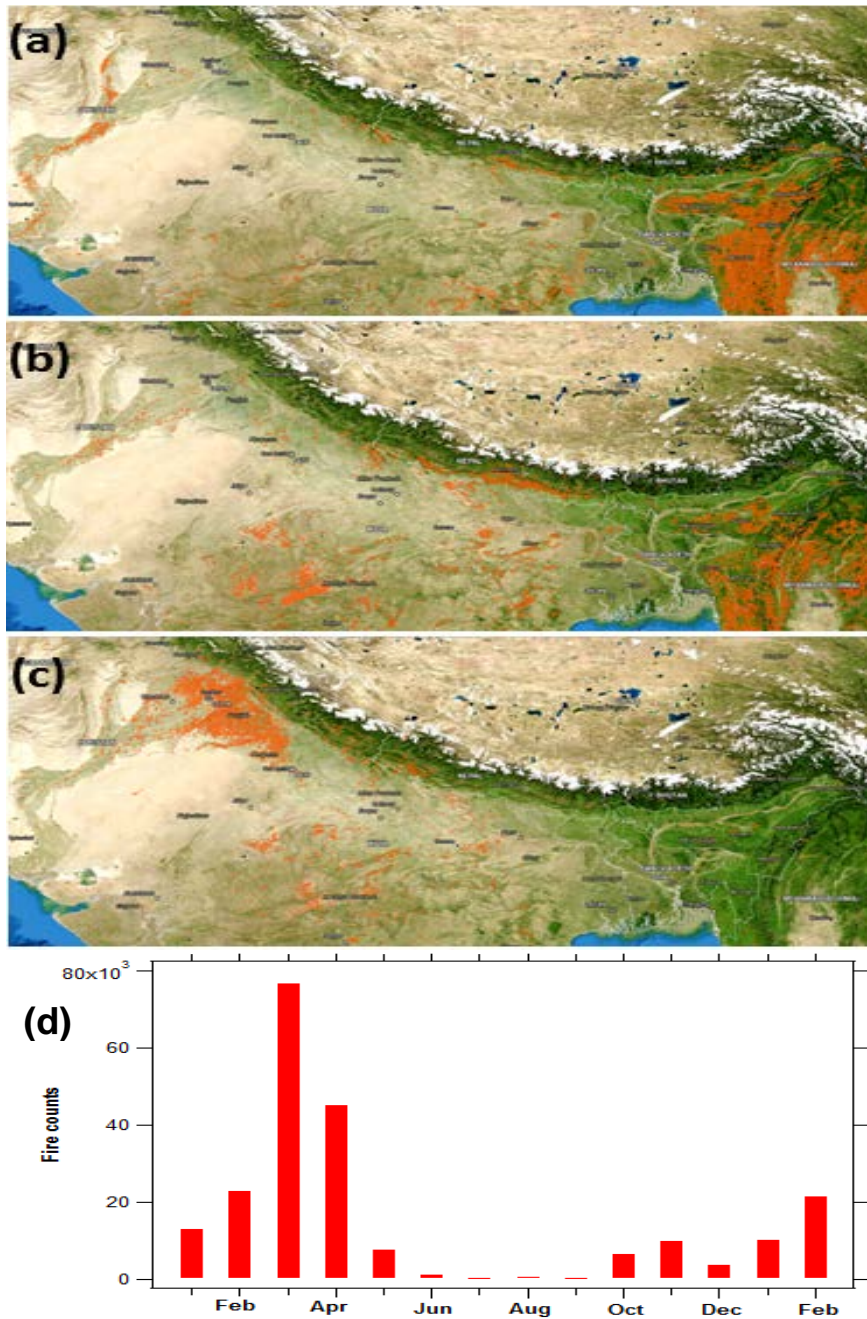


Figure 5. Satellite detected fire counts in (a) Mar, (b) Apr, (c) May 2013 in the broader region surrounding Nepal and (d) total number of fire counts detected by MODIS instrument onboard the Aqua satellite during Jan 2013-Feb 2014. Source: <https://firms.modaps.eosdis.nasa.gov/firemap/>

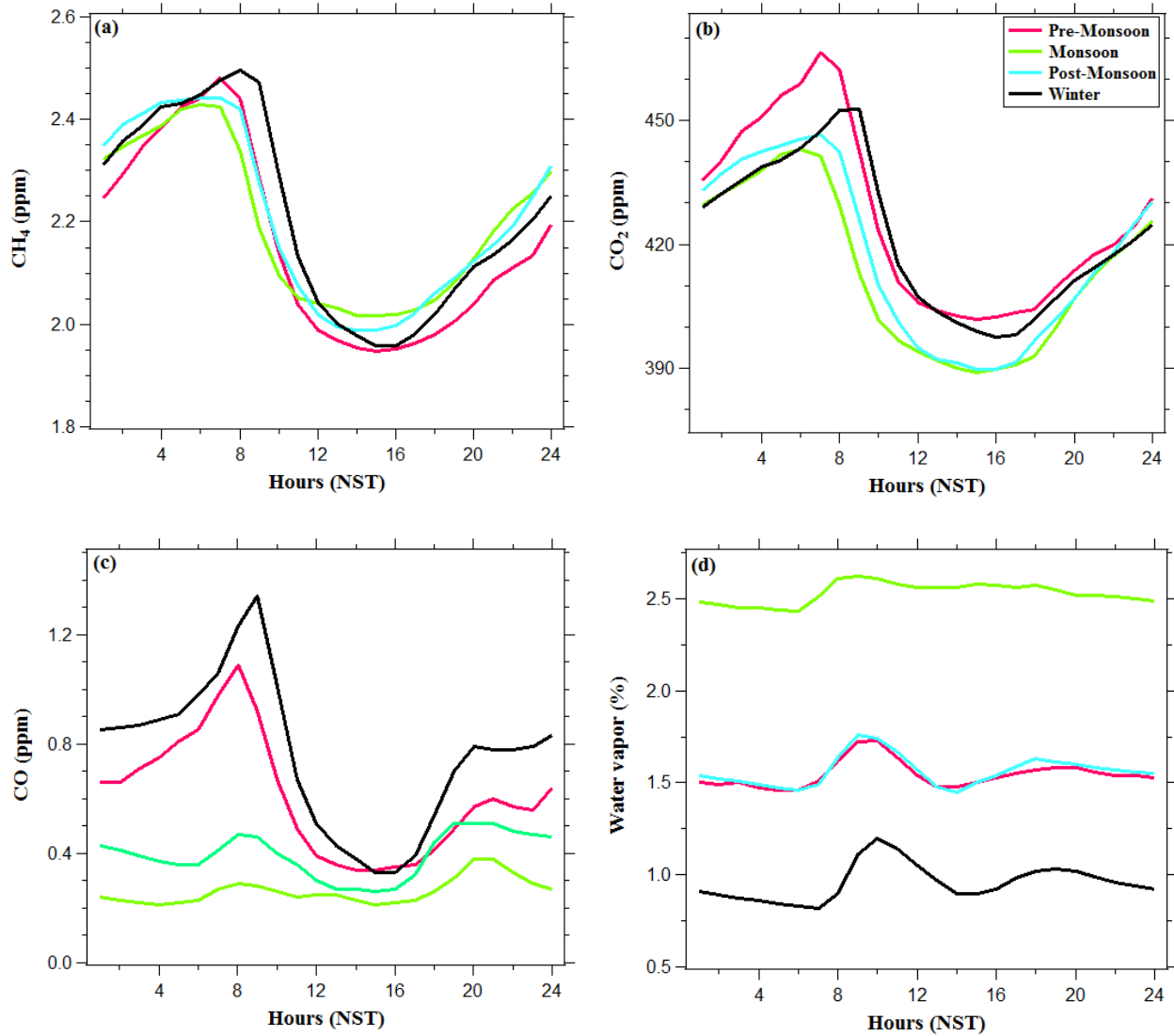


Figure 6. Diurnal variations of hourly mixing ratios in different seasons (a) CH₄, (b) CO₂, (c) CO, and (d) water vapor observed at Bode (semi-urban site) in the Kathmandu Valley during March 2013-February 2014. Seasons are defined as Pre-monsoon: Mar-May, Monsoon: Jun-Sep, Post-monsoon: Oct-Nov, Winter: Dec-Feb. The x axis is in Nepal Standard Time (NST).

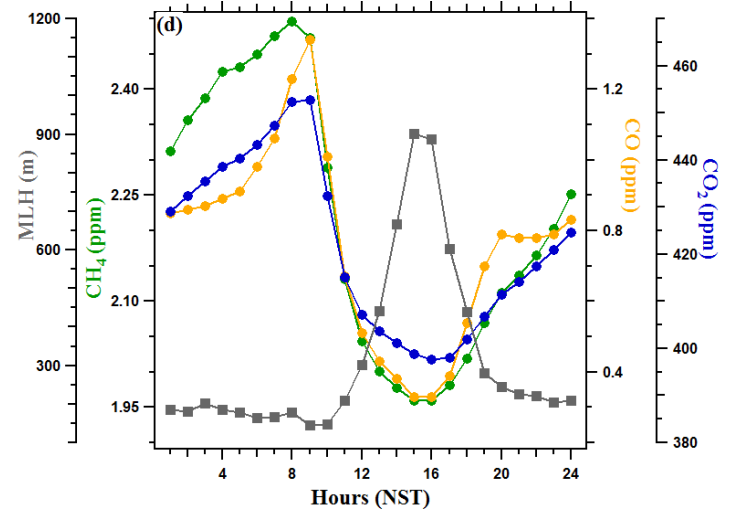
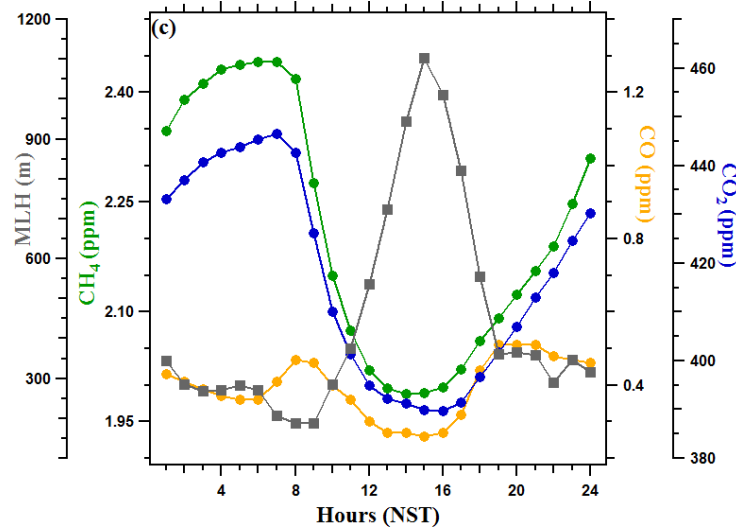
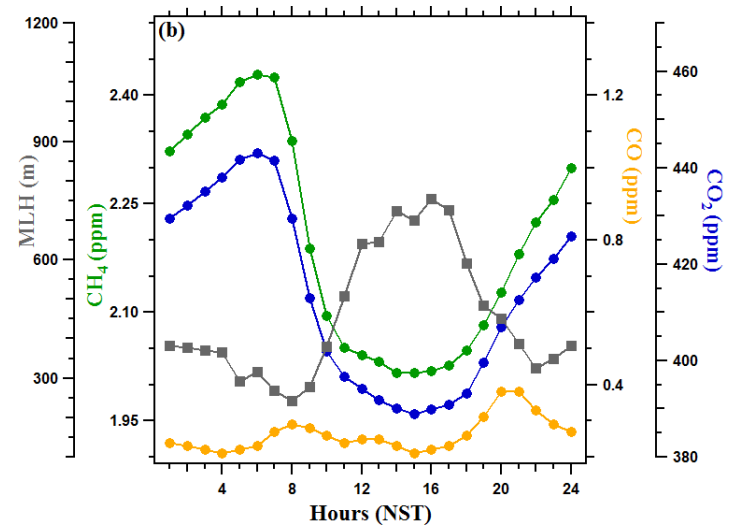
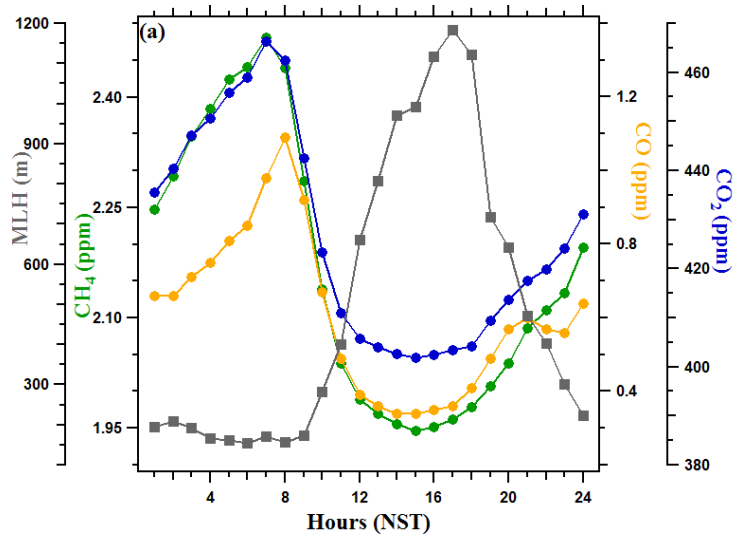


Figure 7. Diurnal variations of hourly mixing ratios of CH₄, CO₂, CO, and mixing layer height (MLH) at Bode (a semi-urban site in the Kathmandu Valley) in different seasons (a) pre-monsoon (Mar-May), (b) monsoon (Jun-Sep), (c) post-monsoon (Oct-Nov) and (d) winter (Dec-Feb) during March 2013- Feb 2014.

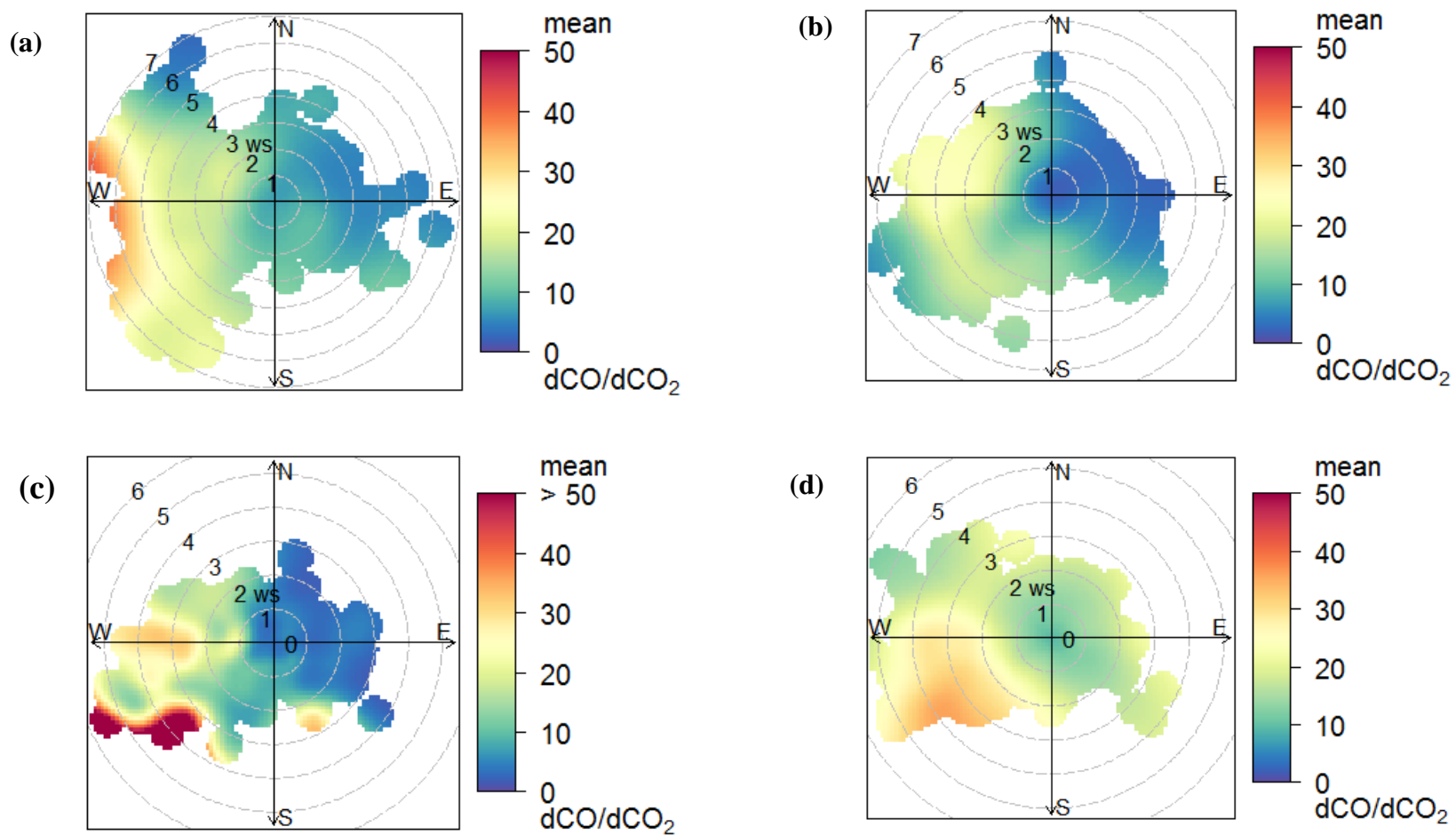


Figure 8. Seasonal polar plot of hourly dCO/dCO_2 ratio based upon wind direction and wind speed: (a) pre-monsoon, (b) monsoon, (c) post-monsoon and (d) winter seasons.

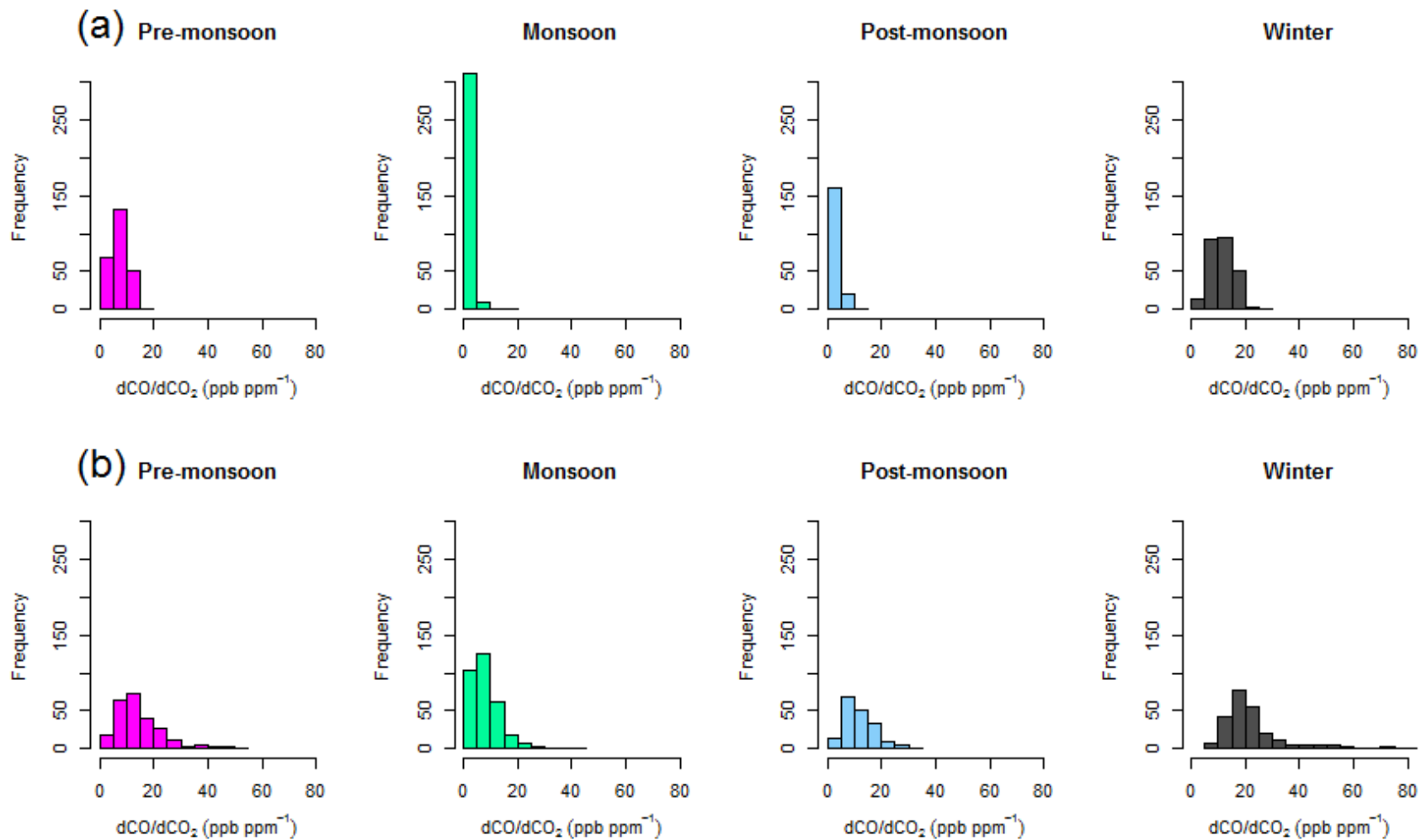


Figure 9. Seasonal frequency distribution of hourly dCO/dCO₂ ratio (a) morning hours (7:00-9:00) in all season except winter (8:00-10:00), (b) evening hours (19:00-21:00)

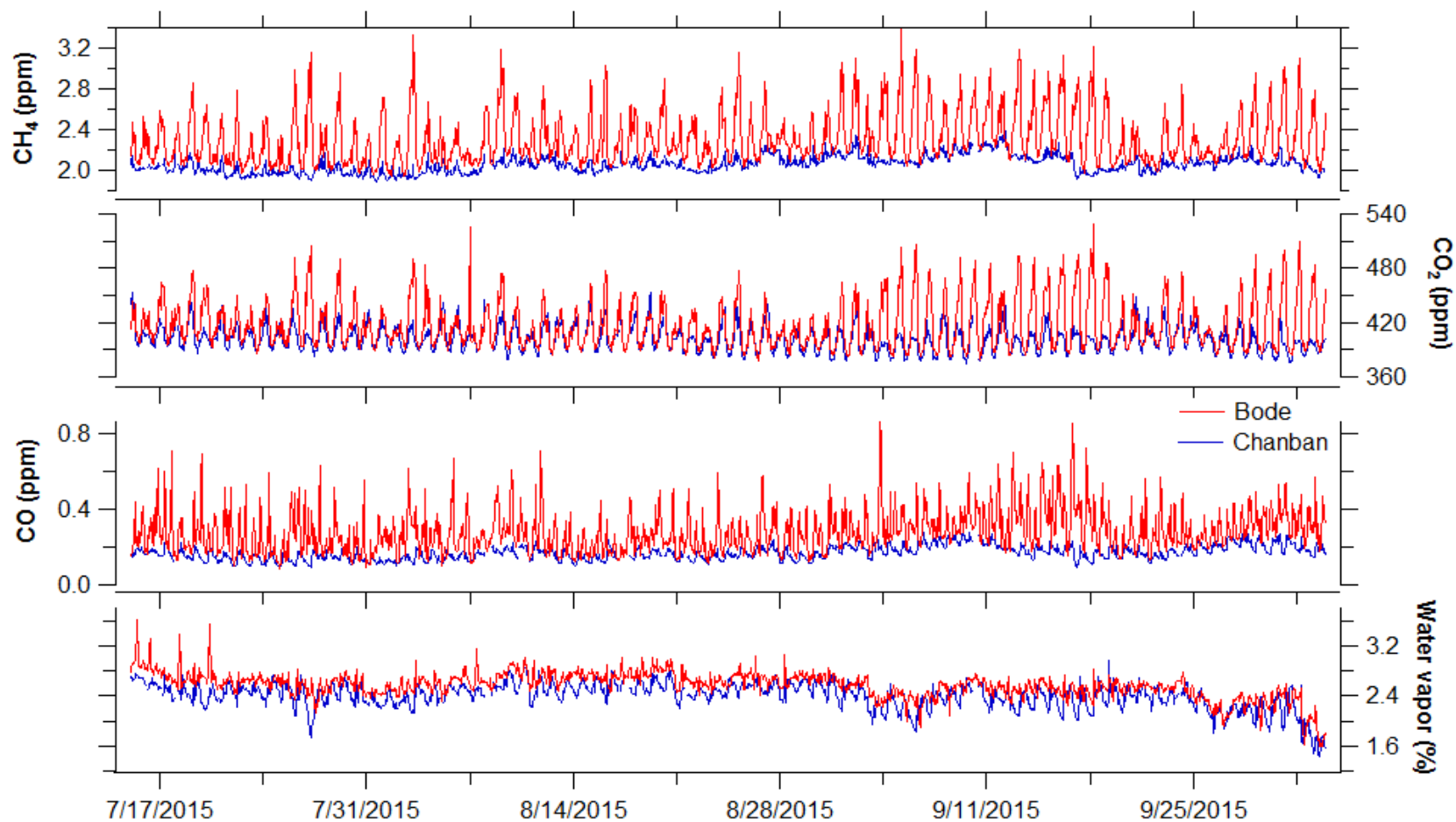


Figure 10. Comparison of hourly average mixing ratios of CH₄, CO₂, CO, and water vapor observed at Bode (a semi-urban site) in the Kathmandu Valley and at Chanban (a rural/background site) in Makawanpur district, ~ 20 km from Kathmandu, on other side of a tall ridge.

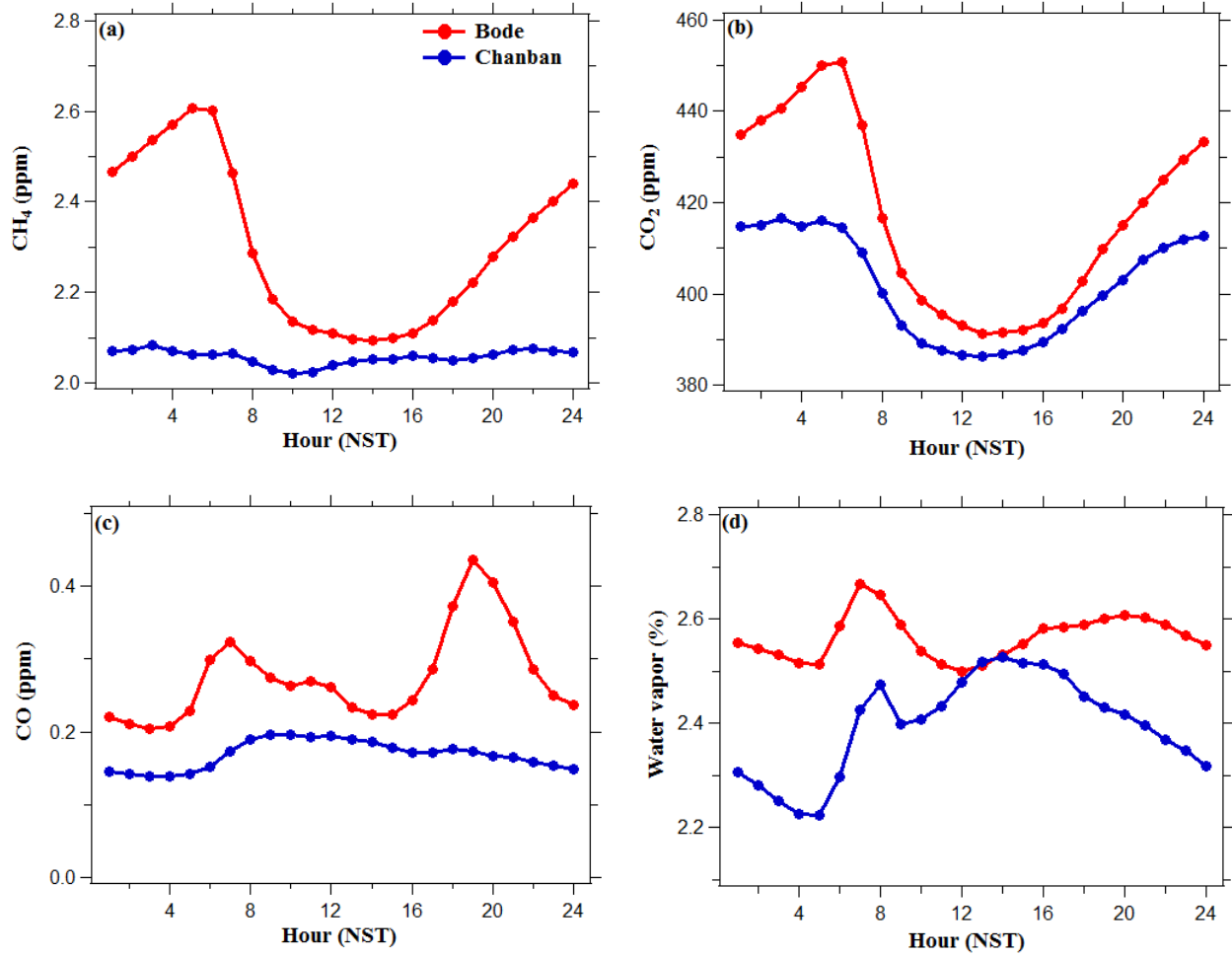


Figure 11. Diurnal variations of hourly average mixing ratios of (a) CH_4 , (b) CO_2 , (c) CO and (d) water vapor observed at Bode in the Kathmandu Valley and at Chanban in Makawanpur district during 15 July- 03 October 2015.